Oxygen Isotopes in Zircon

John W. Valley

Department of Geology & Geophysics
University of Wisconsin
Madison, Wisconsin 53706

valley@geology.wisc.edu

INTRODUCTION

Isotopic and trace element analysis of zircons can provide reliable and robust estimates of age, compositions of coexisting minerals and melts, and constraints on the genesis and protoliths of host rocks. Recent technological developments facilitate analysis of oxygen isotope ratios in zircon with high accuracy and precision by laser heating/ gas-source mass-spectrometry and *in situ* from thin sections or grain mounts by ion microprobe/ secondary ion mass-spectrometer. A large number of studies have shown that non-metamict zircons preserve their $\delta^{18}O$ value from the time of crystallization; hence oxygen isotope ratio can be correlated with age (U-Pb) or trace element composition. The zircon $\delta^{18}O$ record is generally preserved despite other minerals that have been reset by high-grade metamorphism or intense hydrothermal alteration. Thus the refractory nature and robust inheritance of zircon offers a potential means to sort out magmatic equilibration and reequilibration, and post-magmatic alteration, an eternal problem for igneous rocks. New processes and interpretations for igneous events have been proposed when the effects of post-magmatic exchange are fully recognized. Crustal recycling can be recognized from magmatic values of $\delta^{18}O$(zircon), and if source rocks are igneous and young at the time of melting, $\delta^{18}O$ will often be the best geochemical signature.

ANALYSIS OF $\delta^{18}O$ IN ZIRCON

Microanalytical techniques are increasingly useful for stable isotope analysis of silicates. Both the laser fluorination/ mass-spectrometer and the ion microprobe/ secondary ion mass-spectrometer offer significant advantages over conventional techniques for analysis of zircon.

Laser fluorination

Accurate analysis of $\delta^{18}O$ in refractory minerals such as zircon is optimized by use of a CO_2 laser (λ = 10.6 μm). The best precision has been obtained when zircons are powdered before analysis. Accuracy and precision of ±0.05 to ±0.1‰ (1 standard deviation = 1sd) are reported for homogeneous samples of ~2 mg (~0.5 mm^3) (Valley et al. 1994, 1995). For the range of normal igneous zircon grain sizes, 2 mg represents a population of ten to several hundred crystals. The separation and selection of zircons is discussed below and can affect the quality of data. For large zircons, core to rim analytical transects are possible at ~500 μm spatial resolution using a thin diamond saw blade (Valley et al. 1998b). For large single crystals of zircon, in situ analysis by excimer laser (KrF at λ = 248 nm and ArF at 193 nm) has yielded precision as good as ±0.12‰ from ~300 μm spots (Wiechert et al. 2002).

Ion microprobe

Significantly enhanced spatial resolution for oxygen isotope analysis is obtained *in situ* from single zircon crystals in grain mounts or thin sections by use of an ion microprobe (Eiler et al. 1997, Valley et al. 1998a, Peck et al. 2001). Analytical precision for $\delta^{18}O$ of 0.5‰ can be obtained from ~3 ng samples (10 to 20 μm diameter spot, ~600 μm^3) by single collecting, small radius ion microprobe at high-energy offset. New multi-collecting, large radius instruments offer enhanced counting

1529-6466/03/0053-0013$05.00

efficiency and precision a factor of 2 or more better for similar spot sizes (McKeegan and Leshin 2001).

Figure 1 shows a large mm-size zircon megacryst J1-1 from Zwaneng kimberlite that has been micro sampled for laser fluorination and analyzed *in situ* at high mass-resolution with dual Faraday collectors on a Cameca 1270 ion microprobe (Valley and McKeegan, unpublished 2000). The two laser analyses consumed the top half of the crystal and yielded $\delta^{18}O = 4.69‰$. The 31 analyses by ion probe made shallow pits (1-3 mm) represented by the dots and average $\delta^{18}O = 4.49‰$. The agreement of the two techniques demonstrates accuracy approximately equal to precision on the homogeneous KIM-5 zircon standard (Table 1). In J1-1, intracrystalline zonation at the 0.1‰ level correlates with trace element zonation seen by electron microprobe analysis and imaged by cathodoluminescence (Fig. 1a). This is a dramatic improvement over the mg-size samples required by laser fluorination. This high spatial resolution for $\delta^{18}O$ is competitive with that of elemental analysis by electron microprobe, and brings the length scales of oxygen diffusion for igneous and metamorphic processes within the reach of stable isotope analysis. It also opens the door for investigation of zircon overgrowths and other intramineral variation within a sample.

Standards

Table 1 summarizes data for zircon standards that have been analyzed for $\delta^{18}O$ by laser fluorination at the University of Wisconsin Stable Isotope Lab. Many of these zircons have been used as an ion microprobe standard for age or oxygen isotope ratio. Ion microprobe analysis indicates that Aber, J1-1, KIM-2, KIM-5, Mog, and 91500 are homogeneous at the 1‰ level; however more recent high precision analysis shows zonation in J1-1 at the 0.1‰ level (Fig. 1). Zircon 91500 has been the subject of inter-lab comparisons for oxygen isotope ratio by laser fluorination and ion microprobe, as well as age (U-Th-Pb, Lu-Hf), and major, minor, and trace

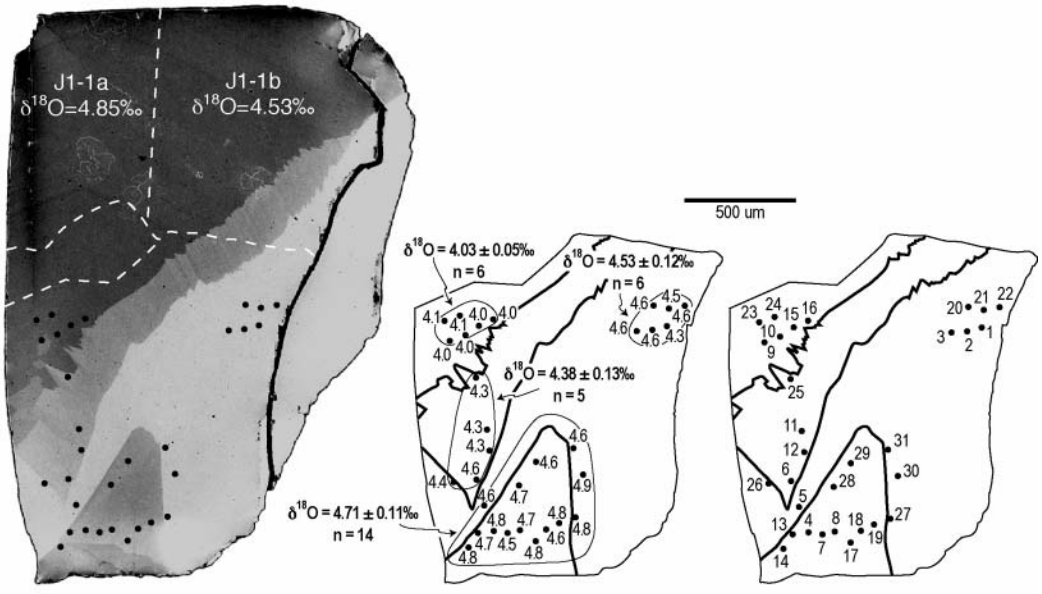

Figure 1. Ion microprobe analyses (dots) of $\delta^{18}O$ in a polished zircon. The top two pieces of the crystal (left) were separated for laser/fluorination; $\delta^{18}O = 4.7‰$ (Valley et al. 1998b). All three images show the remaining bottom piece of the crystal. The spot to spot precision is 0.1‰ (1sd) for 31 consecutive *in situ* analyses of $\delta^{18}O$ requiring about four hours by double-collecting Cameca 1270 (center). The order of analysis (right) was randomized to prevent systematic error. Note that the crystal is zoned in cathodoluminescence (left) due to variable trace element content and that $\delta^{18}O$ correlates with CL zoning (Valley and McKeegan, unpublished 2000).

element content (Wiedenbeck et al. 1995, Wiedenbeck et al. in prep.).

Accurate ion microprobe analysis depends on alternating analysis of samples and homogeneous standards. The instrumental mass fractionation (IMF) varies from about 0 to 40‰ / AMU depending on instrument type, operating conditions and mineral matrix. Routine attainment of the highest accuracy and precision will require optimization of these factors. The matrix correction is relatively small if zircon samples are compared to zircon standards. Nevertheless, Peck et al. (2001) report five zircon standards with variable HfO_2 suggesting that IMF varies about 1‰ / 1 wt % HfO_2, in good agreement with data from Eiler et al. (1997) for orthosilicates (Fig. 2). Over the relatively narrow range of hafnium content in normal igneous zircons (0.5-2.5 wt % HfO_2), this correction will be minor if an appropriate standard of the same composition is used, but chemical composition should be verified by electron microprobe as up to 26 wt % HfO_2 occurs in zircons from pegmatites (Fontan et al. 1980, Speer 1982).

For analysis of $\delta^{18}O$ in zircon by laser fluorination / mass-spectrometry, there is no mineral specific fractionation and it is not necessary to standardize with another zircon. The UWG-2 standard, Gore Mountain garnet, has been used to monitor all analyses of zircon at the Wisconsin Laboratory (Valley et al. 1995). This originally ~2 kg crystal is homogeneous in $\delta^{18}O$, easy to react by laser, yet completely resistant to pre-fluorination at room temperature (Table 1).

ZIRCON SAMPLE PREPARATION

Zircon overgrowths, inheritance of multiple generations of zircon in a single sample, and radiation damage all present possible challenges to oxygen isotope studies. A variety of approaches are available to overcome potential problems through separation, preparation, imaging, and selection of zircons for analysis. The choice of correct procedure depends on the nature of the sample and the analytical technique. These procedures may be necessary for correct interpretation of laser fluorination data where multiple zircons are analyzed in bulk, but sample selection and imaging offer significant advantages for *in situ* analysis as well.

Table 1. Oxygen isotope ratio of zircon, baddeleyite, and garnet standards analyzed by laser fluorination at the University of Wisconsin.

Standard	$\delta^{18}O$ ‰ SMOW	± 1SD	N	age Ma	U ppm	HfO_2 wt.%	Refs.	Comments
						ZIRCON		
Aber	5.05	0.05	3			0.75	3	USNM #83829, Abercrombie R., NSW, Australia
BR231	9.81	0.04	3	571	772	1.30	4, 9	1.8g xt
G168	10.93	0.12	2	547	1499	1.21	4, 9	1.1g xt
J1-1, Jwan	4.69	0.11	2	2643	14	0.93	1, 2	3mm xenocryst, kimberlite, Jwaneng, Botswana
KIM-1	5.20	0.02	2				1	10mm xenocryst, kimberlite, Kimberley, S.A.
KIM-2	5.62	0.09	2			1.04	1,2	10mm xenocryst, kimberlite, Kimberley, S.A.
KIM-3	5.26	0.05	2				1	10mm xenocryst, kimberlite, Kimberley, S.A.
KIM-4	5.33	0.08	2				1	10mm xenocryst, kimberlite, Kimberley, S.A.
KIM-5	5.09	0.06	16			1.23	1, 3	10mm xenocryst, kimberlite, Kimberley, S.A.
Mog	22.94	0.21	5			1.03	3	USNM #R18113, placer, Mogok, Burma
UW-MT	5.03	0.10	2				4	Mud Tank carbonatite, Australia
R33	5.55	0.04	3	419			4, 8	monzodiorite, Braintree complex, Vermont, USA
Temora-1	7.93	0.04	3	417			4, 8	gabbroic diorite, Temora, NSW, Australia
Temora-2	8.20	0.01	3	417			4, 8	gabbroic diorite, Temora, NSW, Australia
91500	10.07	0.03	7	1065	81	0.66	4, 5	syenite gneiss, Renfrew, Ont., 238 g xt
						BADDELEYITE		
Phalabora	3.2	1.5	6	2060	310		4, 10	6cm xt w/apatite, Phalaborwa carbonatite, S.A. Heterogeneous in $\delta^{18}O$
						GARNET		
UWG-1	6.3	0.13	~500				6	garnet amphibolite, Gore Mtn, NY, discontinued use after 1994, also called UWGMG
UWG-2	5.80	0.15	1081				7	~2000g xt, Gore Mtn, NY, 1SE=±0.005‰

References: (1) Valley et al. 1998b, (2) Eiler et al. 1997, (3) Peck et al. 2001, (4) University of Wisconsin, Stable Isotope Lab., unpublished data (5) Wiedenbeck et al. 1995, (6) Valley et al. 1994, (7) Valley et al. 1995, (8) L. Black, pers. comm. 2001, (9) Kennedy 2000, (10) Reischmann 1995.
1 SD: standard deviation. When N=2, 1/2 of the difference is cited.

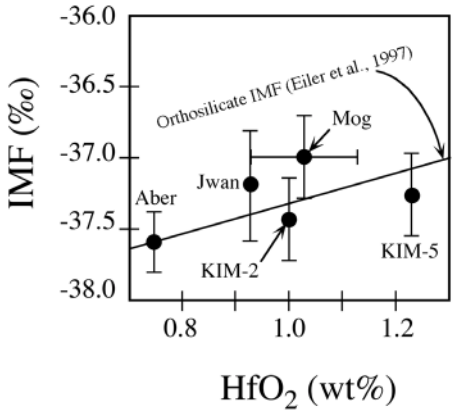

Figure 2. Instrumental mass fractionation (IMF) for ion microprobe analysis of $\delta^{18}O$ in zircon with known HfO_2 content. The orthosilicate IMF (line) was independently determined by Eiler et al. (1997). These data show that Hf substitution measurably affects data correction (from Peck et al. 2001).

Mechanical separation of zircons

Many procedures for separation of zircons from host rock are well known from geochronology studies, including grinding, acid dissolution of other minerals, hydrodynamic separation by Wilfley or gold table, heavy liquids, Frantz magnetic separator, and hand picking under a binocular microscope. Air abrasion is commonly applied to remove high uranium outer regions in igneous zircons and metamorphic overgrowths in order to improve concordance in geochronology (Krogh 1982a). Recently, the removal of rims by air abrasion of a population of small volcanic zircons permitted analysis by laser of the residual cores and the discovery, later confirmed by ion microprobe, that zircons were zoned core to rim by up to 5‰ in $\delta^{18}O$ (Bindeman and Valley (2000a, 2001, 2003).

A relatively new and very promising approach to zircon separation is the Electric Pulse Disintegration (EPD), which uses spark discharges of >100 kV to disaggregate a rock, largely along grain boundaries (Rudashevsky et al. 1995, Saint-Eidukat and Weiblen 1996). This technique can preserve delicate features in igneous, metamorphic, or sedimentary rocks. Cavosie et al. (2002) used EPD to disaggregate a sample of the Jack Hills metaconglomerate and they found a 4.33 Ga zircon core with an intact 3.7 Ga overgrowth. This is the earliest example of crustal recycling known. It is possible that similar overgrowths once existed on a 4.404 Ga zircon from this same outcrop (Wilde et al. 2001), but were broken off during mechanical crushing and grinding.

Selection of zircons

Once zircons are separated and concentrated, they can be sorted and specific populations selected for analysis. Full strength cold HF vigorously dissolves metamict zircon, but crystals with a low degree of radiation damage are not dissolved. This approach is avoided for geochronology because of potential lead loss, but it has been shown to be effective in removing contaminants, inclusions, and radiation damaged portions of zircon with no effect on the $\delta^{18}O$ of good crystalline material (King 1997, King et al. 1998b). Dissolution of crack-healing material can cause zircons to fall apart into shards of relatively fresher zircon.

Use of the Frantz magnetic separator was pioneered by Silver (1963) to concentrate zircons for geochronology (Krogh 1982b). Zircons with the lowest magnetic susceptibility tend to have the lowest concentration of uranium and to be most concordant on a Wetherill concordia diagram (Fig. 3). The uranium-rich zircons have suffered more radiation damage. This can cause the crystal to be crazed with microfractures due to hydration and swelling of damaged uranium-rich domains. Radiation damage also enhances diffusion and exchange of oxygen by creation of fast pathways of exchange, which can short-circuit slower volume diffusion. Analysis of different magnetic fractions of zircon from metamorphosed igneous rocks of the Adirondack Mountains shows that alteration of $\delta^{18}O$ can occur in less concordant samples, that presumably are radiation damaged, though many are not measurably affected (Fig. 4). In extreme cases of radiation damage, metamictization and microfracturing are common, facilitating late exchange of oxygen through short path-length diffusion in damaged material and precipitation of new phases in cracks. Bibikova et al. (1982) also found that metamict zircons are altered and have low $\delta^{18}O$ values. Magnetic separation of zircons

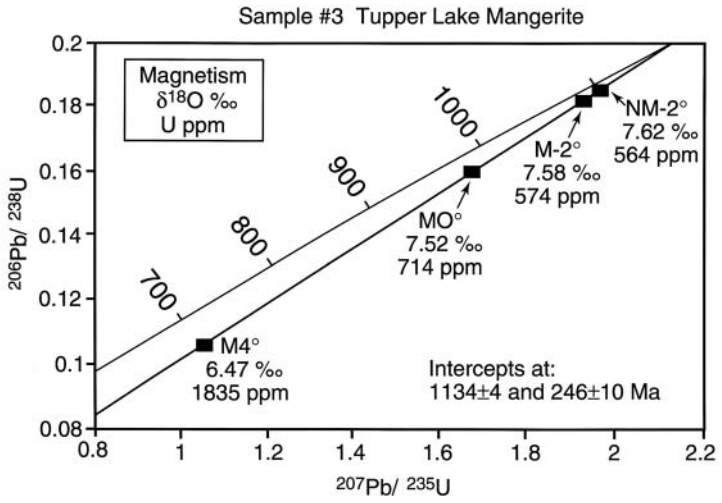

Figure 3. Concordia diagram for magmatic zircons from granulite facies, orthopyroxene-bearing monzonite (mangerite) from the Adirondack Highlands. Zircons were divided by Frantz magnetic separator from lowest to highest magnetic susceptibility (NM-2 < M-2 < M0 < M4). Lower magnetism correlates perfectly with more concordant ages, lower U content, and higher $\delta^{18}O$(Zc). The $\delta^{18}O$ of the least magnetic zircons (7.6‰) is consistent with magmatic $\delta^{18}O$ for the entire AMCG suite in the Adirondack Highlands, while the most magnetic and U-rich zircons are erratic and shifted in $\delta^{18}O$. In thin section, these isotopically shifted zircons are seen to be crazed by microfracture, presumably due to radiation damage resulting from high U and Th content. Such damaged zircons do not withstand HF treatment and should be removed from studies of magmatic $\delta^{18}O$ (data from Valley et al. 1994).

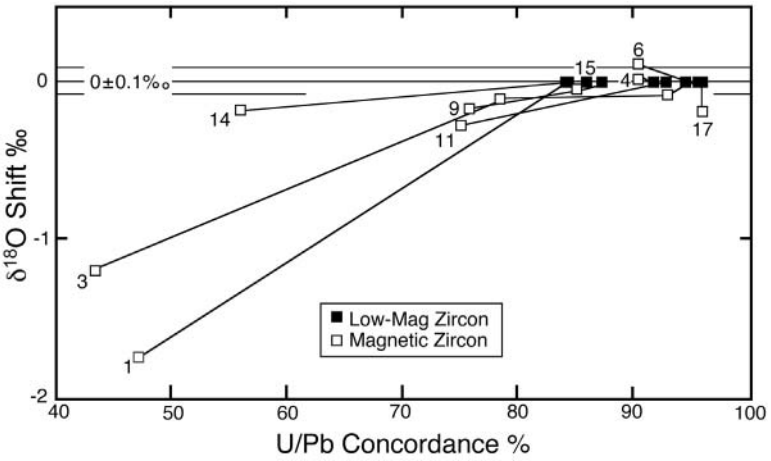

Figure 4. Percent concordance of U-Pb ages vs. shift in $\delta^{18}O$ for magmatic zircons from the Adirondack Mountains. Shift in $\delta^{18}O$ is normalized to $\delta^{18}O$ of the lowest magnetic fraction from a single sample, which is inferred by independent tests to be the primary magmatic $\delta^{18}O$ value. Some magnetic zircons have exchanged $\delta^{18}O$ during retrogression while others are not affected. Post magmatic exchange also correlates with higher U and Th content, and more radiation damage and microfractures (from Valley et al. 1994).

can remove metamict grains and is also an effective means to avoid crystals that contain inclusions of other more magnetic minerals (e.g., magnetite, monazite).

Size and shape are useful properties for selecting zircons. Analysis of sieved zircons from granites on the Isle of Skye, Scotland showed that large and small zircons have the same $\delta^{18}O$ values suggesting that intense hydrothermal alteration had no measurable effect on zircons (Monani and Valley 2001). In contrast, Bindeman and Valley (2000a, 2001) measured crystal size distributions

(CSD) of zircon separates from rhyolites at Yellowstone and analyzed $\delta^{18}O$ in large and small crystals (see Bindeman 2003). They found up to several per mil variation due to growth zoning and exchange in an evolving low $\delta^{18}O$ magma. They also compared CSDs for zircons separated by conventional crushing and Wilfley table separation to zircons obtained by wholesale dissolution of kilogram-size samples of tuff in HF. The CSDs are similar indicating that smaller zircons were not preferentially lost in the conventional procedure. Peck et al. (2003a) separated zircons by size (40 to 180 μm diameter) from granulite facies quartzite and granitic gneiss in order to empirically calibrate the rate of oxygen diffusion in zircon (discussed below).

Imaging zircons

Zircon grains can be viewed and imaged by many techniques. Surprising new information about color, inclusions, zoning, or alteration can result from differences in optical illumination: binocular vs. petrographic microscope, light vs. dark field illumination, plain vs. crossed polarization, immersion in R.I. liquids vs. air, or differential (Normarski) interference contrast. Polished grain mounts or thin sections can also be imaged by cathodoluminescence (CL), backscattered electrons (BSE), and secondary electrons by electron microprobe or SEM, and minor to trace element compositions can be mapped be electron probe (Hanchar and Miller 1993, Hanchar and Rudnick 1995, Fournelle et al. 2000). For larger zircons, a cold cathode luminoscope mounted on a petrographic microscope is useful.

Radiation damage can be imaged in polished surfaces of zircon by fuming with HF vapor (Krogh and Davis 1975). Laser Raman spectroscopy provides a quantitative measure of radiation damage from spots of 1 μm or larger (Wopenka et al. 1996, Nasdala et al. 2001, Balan et al. 2001, Geisler et al. 2001, Geisler and Pidgeon 2001).

OXYGEN ISOTOPE FRACTIONATION IN ZIRCON

The fractionation of oxygen isotopes among zircon and other phases has been estimated from: experiments (Sessions et al. 1996, 2003; Krylov et al. 2002); theoretical calculations based on spectroscopy (Kieffer 1982) or electrostatic potential (Smyth 1989); the increment method (Hoffbauer et al. 1994, Richter and Hoernes 1988, Zheng 1993); and by empirical measurements of natural samples (Valley et al. 1994, 2003; King et al. 2001). These varied calibrations are critically

Table 2. Oxygen isotope fractionations between zircon and selected minerals. Values are the $A_{A\text{-}B}$ coefficient from Eqn (1), below, where A and B are minerals from the Y- and X-axes, respectively.

	Cc	Ab	Mu	F-Ph	An	Ph	Ap	Zc	Alm	Di	Gr	Gh	Ttn	Fo	Ru	Mt	Pv
Qt	0.38	0.94	1.37	1.64	1.99	2.16	2.51	2.64	2.71	2.75	3.03	3.50	3.66	3.67	4.69	6.29	6.80
Cc		0.56	0.99	1.26	1.61	1.78	2.13	2.26	2.33	2.37	2.65	3.12	3.28	3.29	4.31	5.91	6.42
Ab			0.43	0.70	1.05	1.22	1.57	1.70	1.77	1.81	2.09	2.56	2.72	2.73	3.75	5.35	5.86
Mu				0.27	0.62	0.79	1.14	1.27	1.34	1.38	1.66	2.13	2.29	2.30	3.32	4.92	5.43
F-Ph					0.35	0.52	0.87	1.00	1.07	1.11	1.39	1.86	2.02	2.03	3.05	4.65	5.16
An						0.17	0.52	0.65	0.72	0.76	1.04	1.51	1.67	1.68	2.70	4.30	4.81
Ph							0.35	0.48	0.55	0.59	0.87	1.34	1.50	1.51	2.53	4.13	4.64
Ap								0.13	0.20	0.24	0.52	0.99	1.15	1.16	2.18	3.78	4.29
Zc									0.07	0.11	0.39	0.86	1.02	1.03	2.05	3.65	4.16
Alm										0.04	0.32	0.79	0.95	0.96	1.98	3.58	4.09
Di											0.28	0.75	0.91	0.92	1.94	3.54	4.05
Gr												0.47	0.63	0.64	1.66	3.26	3.77
Gh													0.16	0.17	1.19	2.79	3.30
Ttn														0.01	1.03	2.63	3.14
Fo															1.02	2.62	3.13
Ru																1.60	2.11
Mt																	0.51

Eqn 1: $1000\ ln(\alpha_{A\text{-}B}) = A_{A\text{-}B}\ (10^6/T^2)$, (T in K). Values should not be extrapolated below ~600°C.
Abbreviations: Ab = albite, Al = almandine, An = anorthite, Ap = apatite, Cc = calcite, Di = diopside, F-Ph = fluorphlogopite, Fo = forsterite, Gh = gehlenite, Gr = grossular, Mu = muscovite, Mt = magnetite, Ph = phlogopite, Pv = perovskite, Qt = quartz, Ru = rutile, Ttn = titanite, Zc = zircon.
Data for Ab, An, Ap, Cc, Di, F-Ph, Fo, Gh, Mu, Mt, Ph, Pv, Qt, and Ru are from solid media exchange experiments with calcite summarized by Chacko et al. (2001). Data for Alm, Gr, Qt, Ttn, and Zc are from empirical calibrations summarized by Valley et al. (2003).

reviewed by Valley et al. (2003).

Self-consistent values for the fractionation of oxygen isotopes between zircon and other minerals come from the empirical calibrations for zircon and experimental studies for other minerals. Table 2 summarizes the empirically derived A coefficients for Equation (1):

$$\delta^{18}O_A - \delta^{18}O_B = \Delta_{A\text{-}B} \approx 1000\ ln\ (\alpha_{A\text{-}B}) = A_{A\text{-}B}\ 10^6 / T^2 \quad (T \text{ in K}) \qquad (1)$$

The largely empirical data sets of King et al. (2001) and Valley et al. (2003) can be combined with results from high-pressure experiments for calcite-mineral exchange summarized by Chacko et al. (2001) to create a matrix of A coefficients for 17 minerals (Table 2). It should be noted that the A coefficient assumes linearity of 1000 lnα vs. $1/T^2$, which is not always observed at low temperatures. These coefficients can be applied above ~600°C, but the specific data source should be evaluated for application at lower temperatures as discussed by Clayton and Kieffer (1991) and Chacko et al. (2001).

OXYGEN DIFFUSION RATE IN ZIRCON

Volume diffusion through the crystal structure is potentially an important mechanism of oxygen exchange in zircon and other minerals (Eiler et al. 1992, 1993; Watson and Cherniak 1997, Kohn 1999, Peck et al. 2003a). Most commonly, this is modeled as exchange involving the entire volume of the entire crystal with flux normal to grain boundary (i.e., rim to core). Other mechanisms including recrystallization, overgrowths, precipitation of material along microfractures, and fast pathways of exchange (inclusions, crystal defects, α- and fission-tracks) can also alter the $\delta^{18}O$ of zircon and cause isotope heterogeneity. However, these mechanisms depend on the details of local geologic environment that are inherently difficult to predict. The presence or absence of such features can generally be evaluated by U-Pb geochronology, imaging, or other tests described above. In contrast, rim to core volume diffusion is more predictable and is always operative, but its rate, which increases with temperature, may be so slow that the effect is neither measurable nor significant.

The rate of oxygen diffusion in zircon has been determined by: laboratory experiments, theoretical calculations, and empirical measurements in metamorphic rocks. These different techniques have yielded widely varying estimates of diffusion coefficient for both high P_{H2O} (wet) and anhydrous (dry) conditions (Fig. 5a).

Watson and Cherniak (1997) measured the rate of oxygen diffusion in zircon under dry (P_{H2O} < 1bar) and wet (P_{H2O} = 70 bar to 10 kbar) experimental conditions using synthetic and natural zircon samples. No anisotropy of diffusion rate was observed in measurements made parallel and perpendicular to the crystallographic *c*-axis. The dry data confirm earlier experiments of Muehlenbachs and Kushiro (1974). Fortier and Giletti (1989) and Zheng and Fu (1998) estimated diffusion rate based on anion porosity, calibrated against experiments for other minerals. Kohn (1999) estimated the effect of water buffering reactions during retrogression.

Both Watson and Cherniak (1997) and Zheng and Fu (1998) found that diffusion is significantly faster at higher P_{H2O}, i.e., "wet" vs. "dry," an effect observed in many minerals (see Cole and Chakraborty 2001). The values of the diffusion coefficient (D) for oxygen, however, vary greatly and with the exception of the dry experiments, there is little agreement among studies (Fig. 5a).

Empirical measurements in high-grade metamorphic rocks provide an independent means to evaluate the rates of oxygen isotope exchange by diffusion (Valley et al. 1994, Peck et al. 2003a). These tests include laser fluorination and ion microprobe analyses of detrital zircons from quartzite and of magmatic zircons from granitic gneisses with known thermal histories. Figure 5b shows values of $\delta^{18}O$ of detrital zircons and metamorphic garnets plotted against $\delta^{18}O$ of the host quartzite. Vertical tie-lines connect analyses for different size fractions of zircon from a single rock. The values of $\delta^{18}O(Zc)$ are similar to those of protolith magmatic zircons throughout the Grenville Province (Peck et al. 2000), while $\delta^{18}O(Qt)$ is similar to the protolith sandstones. None of the twelve

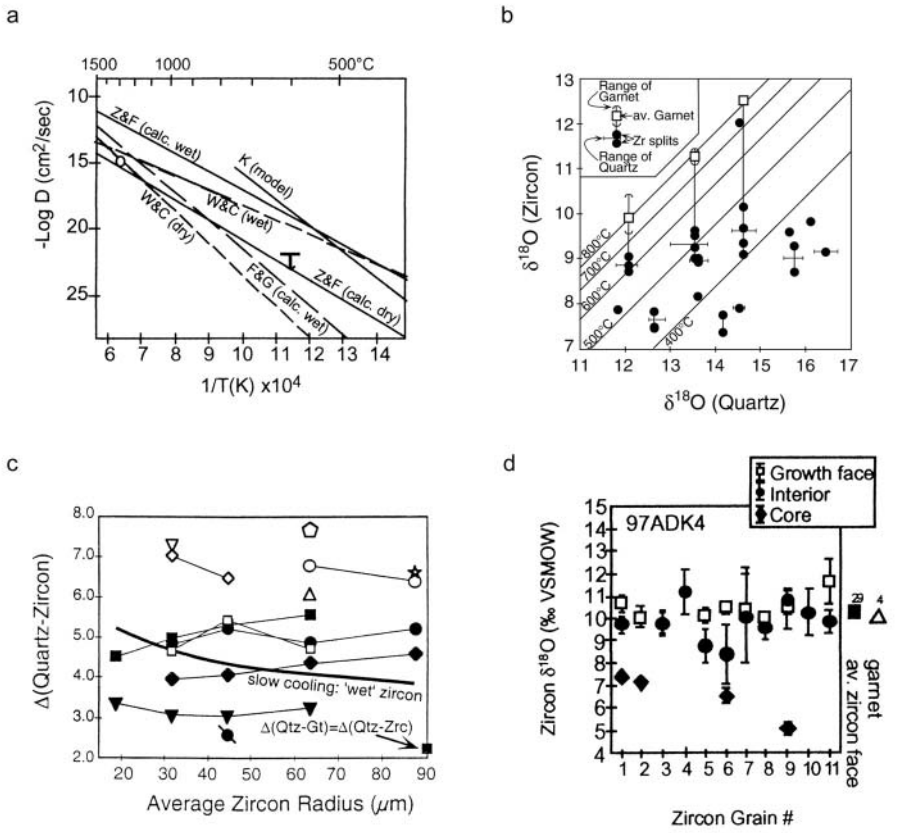

Figure 5. (a) Arrhenius plot of experimentally determined and calculated oxygen diffusion rate in zircon. W&C are experiments by Watson and Cherniak (1997). F&G and Z&F are calculated by Fortier and Giletti (1989) and Zheng and Fu (1998). "K model" is estimated for a cooling metabasite (Kohn 1999). The circle is a dry experiment by Muehlenbachs and Kushiro (1974). The bar with an arrow is an empirical calibration by Peck et al. (2003). (b) Values of $\delta^{18}O$(quartz) vs. $\delta^{18}O$(detrital Zc) from granulite facies Grenville quartzites. Zircons of different size from the same sample are connected with vertical tie-line. Zircons did not equilibrate with host quartz during metamorphism at 675-775°C. In contrast metamorphic garnets are equilibrated. (c) Values of $\Delta^{18}O$(Qt-Zc) vs. zircon crystal size for samples shown in 5b. Predicted relations for slow cooling and "wet" diffusion are shown. The lack of systematic relations with grain size show that zircons neither equilibrated at the peak of metamorphism nor were significantly altered after metamorphism. (d) Ion microprobe analyses of $\delta^{18}O$ from cores and rims of individual detrital zircons from Grenville quartzite 97ADK4. Analyses of grain interiors (filled circles and diamonds) and crystal growth faces (open squares) are shown. The variability of cores demonstrates preservation of premetamorphic magmatic compositions in zircon. The uniformity of data for the outer 3 μm on crystal faces shows exchange and equilibration is restricted to a micron-scale during metamorphism (from Peck et al. 2003a).

rocks containing quartz-zircon pairs have equilibrated at the peak metamorphic temperatures, 675-775°C. In contrast, all three of the quartz-garnet pairs record peak metamorphic temperatures (Peck et al. 2003a). Likewise, Bolz (2001) reports ion microprobe analyses of unexchanged detrital zircons that experienced 700-800°C contact metamorphism of Appin quartzite at Ballachulish, Scotland. Both studies show that zircons preserve premetamorphic values and that little exchange has occurred by diffusion or any other mechanism.

An examination of $\Delta^{18}O$(Qt-Zc) vs. zircon radius for twelve Grenville quartzites (Fig. 5c) reinforces the conclusion that zircons were not significantly affected by oxygen diffusion either

during prograde or retrograde metamorphism. Diffusion modeling allows prediction of the nature and magnitude of exchange, *if* diffusion was an important process for specified conditions. If the input includes D from experiments at $P_{H2O} > 70$ bar (Watson and Cherniak 1997), these calculations predict that zircons will completely equilibrate with quartz at metamorphic temperatures of 675-775°C and that further exchange during slow cooling will affect small zircons more than large zircons because of differences in surface area/ volume. The smooth curve in Figure 5c shows the predicted values of $\Delta^{18}O$(Qt-Zc). None of the twelve rocks follow this trend, predicted for $P_{H2O} > 70$ bar, and many have a different slope. Thus, Peck et al. (2003a) conclude that the lack of equilibrium values in zircon cannot be attributed to retrogression and must indicate preservation of premetamorphic $\delta^{18}O$. Similar calculations are made for values of $\delta^{18}O$(Zrc) measured in granitic gneisses, which are the rock type from which zircons are most commonly studied. The conclusions are similar; zircons do not show correlations predicted if diffusion was significant and the best interpretation is that zircons in granitic gneisses have also preserved approximately the original $\delta^{18}O$ from the time of magmatic crystallization. Clearly, the wet experimental data cannot be used to accurately model the natural processes of exchange in these rocks. However, the data agree with predictions of very much slower diffusion that are made using the data for anhydrous experiments (Watson and Cherniak 1997).

Two quartzites from Figure 5c were chosen for detailed study by ion microprobe (Peck et al. 2003a). Individual zircons were mounted first in acetone-soluble cement for analysis into polished surfaces in the center of the grain. Then crystals were freed, turned over, and remounted by pressing into indium such that the ion microprobe could depth profile into the outer 3 μm of crystal growth faces. These data are shown in Figure 5d. In spite of the larger analytical uncertainty of ion microprobe data, it is clear that the cores and interiors of zircons (diamonds and dots) are significantly lower in $\delta^{18}O$ than the outermost rims (growth faces = squares). The cores show considerable variability, presumably representing the mix of rocks in the sediment source region, while the faces are all the same within analytical uncertainty. The average $\delta^{18}O$(Zc face) is in equilibrium with the metamorphic garnet (triangle) and the host quartz. Thus, thin high $\delta^{18}O$ rims have formed by diffusion at ca. 675°C, but cores were not affected.

Zircon #9 from Figure 5d is shown as a CL image in Figure 6. The location of ion microprobe pits and $\delta^{18}O$ are shown for a polished surface through the crystal core. The inherited core of this crystal (bright CL) has low $\delta^{18}O$ (5.1‰), while the magmatic overgrowth (dark CL) is higher in $\delta^{18}O$ (10.6‰). At the time of magmatic overgrowth this internal boundary was a natural diffusion couple, i.e., a step discontinuity in $\delta^{18}O$, and the gradient is still 5.5‰ across a distance of less than 50 μm. Ion microprobe analysis, described above, suggests that this crystal also has a thin rim that exchanged during metamorphism with surrounding quartz, however, the steepness and the depth within the crystal of the gradient shown in Figure 6 show that it was not caused by metamorphic exchange at 700-800°C with quartz. Instead, the core rep-

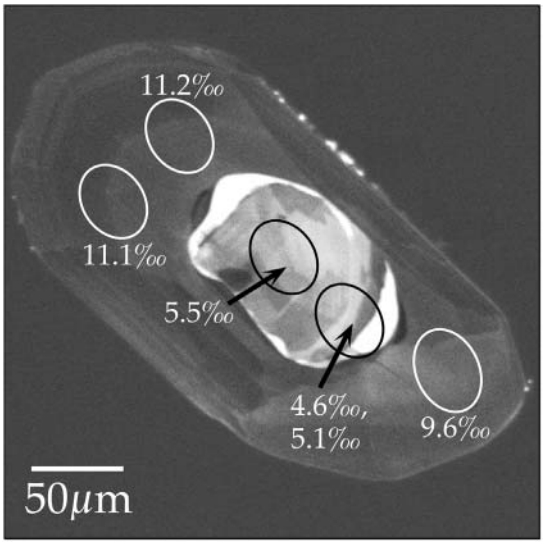

Figure 6. Cathodoluminescence image of detrital igneous zircon #9 from Figure 5d. The $\delta^{18}O$ of the inherited core is distinct from the magmatic overgrowth suggesting that $\delta^{18}O$ was preserved in the zircon core during a period of magmatic resorption and overgrowth that preceded granulite facies metamorphism (from Peck et al. 2003a).

resents a normal $\delta^{18}O$ zircon xenocryst that was inherited by a higher $\delta^{18}O$ igneous magma. The lower $\delta^{18}O$ core was preserved through the magmatic event and subsequent metamorphism due to slow diffusion of oxygen through the zircon.

Diffusion modeling based on the different values of D shown in Figure 5a lead to surprisingly different conclusions. The predicted closure temperature for oxygen diffusion in average-size igneous zircons under conditions of slow cooling is over 900°C using the dry data of Watson and Cherniak (1997), but the temperature is only 500-550°C using their wet data at $P_{H2O} \geq 70$ bar. Peck et al. (2003a) conclude that all available empirical data from quartzites and granitic gneisses support diffusion rates similar or possibly slower than the dry data. It is clear that magmatic zircons can preserve the igneous value of $\delta^{18}O$ through subsequent high grade metamorphism, hydrothermal alteration, and possibly magmatic assimilation or anatexis. This conclusion has been verified by many studies of magmatic zircons that are summarized below.

ASSIMILATION VS. FRACTIONAL CRYSTALLIZATION

Analysis of zircon can provide a test of closed system magmatic crystallization vs. open system assimilation, contamination, or post magmatic alteration. In a simplified hypothetical case; if a suite of mafic to felsic magmas differentiate in a closed system from a common parent by fractional crystallization at constant temperature, then the $\delta^{18}O$ values of zircon crystallizing from each magma will be the same even though the whole rock $\delta^{18}O$ of the felsic magma can be 1-2‰ higher than its mafic sibling. This arises because all phases are assumed to be in equilibrium throughout the process and differentiation progresses by early removal of mafic minerals, which are lower in $\delta^{18}O$ than quartz and feldspar. The whole rock values increase as the percentage of higher $\delta^{18}O$ quartz and feldspar increases, but the Δ(WR-Zc) increases at the same rate for the same reason, and $\delta^{18}O$ is unchanged for each mineral including zircon. Thus, the $\delta^{18}O$(WR) value increases as the percentage of high $\delta^{18}O$ minerals increases. Of course, temperature must decrease for crystallization to progress and the zircon saturation temperature is dependent on composition as well (Watson and Harrison 1983), but the effect of ΔT is not generally significant due to small differences in fractionation at magmatic temperatures.

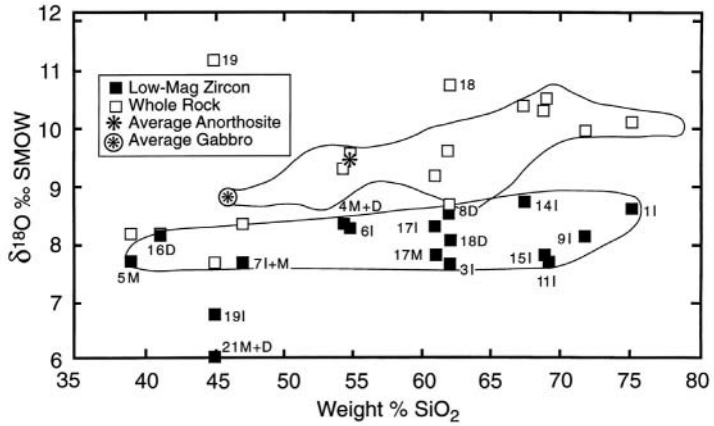

Figure 7. Plot of $\delta^{18}O$(low magnetism zircon) vs. wt % SiO_2 for metamorphosed igneous rocks of the AMCG suite, Adirondack Mountains. All AMCG zircons (SiO_2 = 39-75 %), except in two metagabbros, have constant $\delta^{18}O = 8.1 \pm 0.4$‰. This is over 2‰ higher than in a primitive mantle-derived mafic magma. Whole rock $\delta^{18}O$ increases with SiO_2 due to increasing abundance of high $\delta^{18}O$ minerals, feldspar and quartz. The generally high $\delta^{18}O$ of AMCG zircons results from magmatic processes before the crystallization of zircon (melting of the deep crust and/or contamination). In contrast to zircons, some whole rock compositions have been raised by post magmatic exchange (from Valley et al. 1994).

The assumption of equilibrium must also be evaluated, but appears correct for most simple plutonic systems. In contrast to the simplified model above, if material is added (or subtracted) from the magma, which is not in isotopic equilibrium, then $\delta^{18}O$ of the magma changes, as does $\delta^{18}O$ of subsequently crystallizing minerals including zircon. Changes in magma chemistry are often recorded by growth zoning in zircon. Such core to rim zonation of $\delta^{18}O$ in zircon provides important evidence for the genesis of low $\delta^{18}O$ rhyolites (see below).

Valley et al. (1994) analyzed $\delta^{18}O$ in zircon and whole rock powder from the Proterozoic anorthosite-mangerite-charnockite-granite (AMCG) suite in the Adirondack Mountains, NY (Fig. 7). Values of $\delta^{18}O(Zc)$ are constant at 8.1±0.4‰ (1sd, N = 13) for all but two metagabbro samples. While this uniformity is consistent with differentiation from a common parent, controversy over the relation of anorthosite massifs to their granitic envelope has generally been resolved in favor of a cogenetic, but not comagmatic model (Ashwal 1993). Thus, the two metagabbro samples provide critical evidence (#19, 21; Fig. 7). These rocks are thought to be samples of the anorthosite parent magma and the lower $\delta^{18}O$ (6-7‰) indicates that two differentiation trends exist, a steep one for anorthosite, which included significant contamination by high $\delta^{18}O$ crust, and a flat one for granitic rocks. Except for a few samples affected by post-magmatic exchange, the whole rock values of $\delta^{18}O$ increase regularly with SiO_2 wt % as predicted for the granitic trend. There is no evidence to support the once common misconception that metasom-atism was active during granulite facies metamorphism in these rocks (see Valley et al. 1990, Eiler and Valley 1994).

In rocks that contain more than one refractory magmatic mineral that crystallize at different times, it is possible to track open system contamination. Likewise, if zircon crystallizes over a period of time when magmatic composition changes, then core to rim growth zoning records this change. The contrast of magmatic garnet and zircon from the Idaho batholith is an example of the former test. Values of $\delta^{18}O(Zc)$ throughout the batholith average 6.9±0.9‰ and the fractionation Δ(Gt-Zc) increases regularly with $\delta^{18}O(Zc)$ (Fig. 8). King and Valley (2001) suggest that progressive contamination has caused the increase in $\delta^{18}O$ of both minerals, but that zircon, which crystallized first, is less affected. If the contaminant was a high $\delta^{18}O$ sediment (average Belt series metasediment = 17‰) then the samples where Δ(Gt-Zc) = 0.2‰ represent about 2% contamination, while the higher $\delta^{18}O$ samples with Δ(Gt-Zc)~0.8‰ represent 10% contamination. In a similar study of the Dinkey Dome granite, central Sierra Nevada batholith, Lackey et al. (2002) found that $\delta^{18}O(Zc) = \delta^{18}O$(garnet) representing equilibration in five samples from the western half of the pluton. In contrast, $\delta^{18}O$(garnet) is ~0.5‰ less than $\delta^{18}O(Zc)$ in five samples from the eastern half of the pluton. Since the magmatic garnets crystallized later than zircons, these results indicate contamination of the Dinkey dome granite by low $\delta^{18}O$ material after zircon crystallized. This contamination is not apparent from analysis of $\delta^{18}O(Qt)$ or $\delta^{18}O(WR)$ due to the scatter of these values by post-magmatic alteration. The significance of such trends would be strengthened by garnet thermobarometry in rocks with appropriate mineral assemblages such as

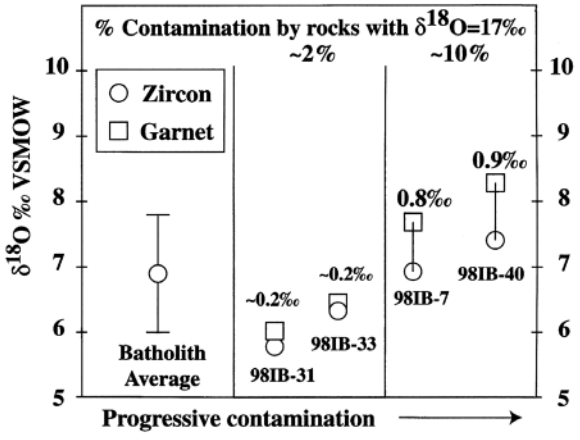

Figure 8. Plot of $\delta^{18}O$ zircon and garnet vs. contamination of granitic magmas in the Idaho batholith. Zircon crystallized earlier than magmatic garnet and thus records the composition of less contaminated magma than garnet. Contamination of magmas by ~10% of high $\delta^{18}O$ rocks such as the Belt Supergroup sediments would raise $\delta^{18}O$(magma) by ~0.9‰ (from King and Valley 2001).

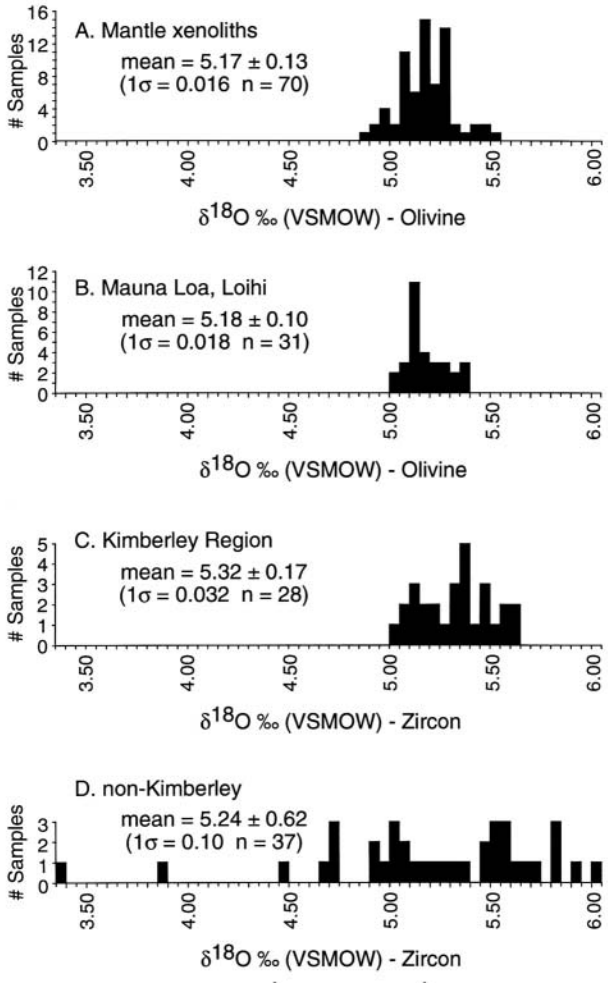

Figure 9. Values of $\delta^{18}O$ for olivine and zircon from mafic and ultramafic rocks. Zircon megacrysts from kimberlite (C) are in high temperature equilibrium with olivine from peridotite xenoliths (A) and oceanic basalts (B). The $\delta^{18}O$ of zircon in equilibrium with the mantle is thus 5.3±0.3‰ (from Valley et al. 1998b).

garnet + biotite or garnet + clinopyroxene, which fixes temperature, or garnet + aluminosilicate + plagioclase + quartz or garnet + quartz + pyroxene + plagioclase, which fixes pressure.

MANTLE ZIRCONS

A distinctive suite of zircon megacrysts occurs in kimberlite at trace amounts (ppm) and are separated during diamond mining (Kresten et al. 1975, Valley et al. 1998b). Typically, these crystals are large (mm to cm), U-poor (<50 ppm), fractured, and coated with ZrO_2 (baddeleyite or tetragonal zirconia, Kresten et al. 1975). In most cases, the U-Pb age matches kimberlite magmatism. These characteristics identify megacrysts as mantle-derived and similar to zircons found associated with diamond, coesite, and other mantle material.

The mantle zircon megacrysts from kimberlite pipes near Kimberley, South Africa are remarkably constant in $\delta^{18}O$ (Fig. 9C) indicating a mantle value of 5.3±0.3‰ (2 sd, Valley et al. 1998b). The mantle zircon value is 0.15‰ higher than $\delta^{18}O$ measured for olivine from mantle xenoliths (Fig. 9A; Mattey et al. 1994) or from most ocean island basalts (Fig. 9B; Eiler et al. 1996), consistent with equilibration at mantle temperatures.

Zircons from kimberlites on the Siberian platform are slightly more variable than in S. Africa, with averages varying from 4.73±0.01‰ at Chomurdakh to 5.53±0.06‰ at Mir. While the analyzed sample set is small, the homogeneity at each pipe is striking, suggesting small, but significant regional differences in the $\delta^{18}O$ of mantle melts (Valley et al. 1998b).

Two suites of zircon megacrysts are found at Zwaneng, Botswana. One has Permian U-Pb ages (the eruption age of the pipe) and the other has Precambrian ages (Kinny et al. 1989). Eight Permian zircons are homogeneous at $\delta^{18}O$ = 5.74±0.13‰; however the Precambrian zircons are the only suite that has been found thus far to show significant variability, $\delta^{18}O$ = 3.37-4.72 (Valley et al. 1998b). One Precambrian zircon has been analyzed in detail by ion microprobe revealing that variability of 0.7‰ exists within the 3 mm crystal and correlates with zoning seen by cathodoluminescence (Fig. 1) suggesting growth zonation. While the Precambrian Zwaneng zircons are interpreted as mantle megacrysts (Kinny et al. 1989), it can be questioned if they have had an extended history in the crust as oxygen isotope zonation would be expected to homogenize by diffusion over 2 billion years at mantle temperatures. Values of $\delta^{18}O$ = 4.78±0.16 are also lower than normal for mantle zircon megacrysts from alkali basalts at Elie Ness, Scotland (Upton et al. 1999). These lower values suggest the burial of hydrothermally altered sea floor basalts into the mantle source regions for alkalic magmas.

PRE-CAMBRIAN ZIRCONS

Archean granitoids

The Superior Province is the largest Archean craton in the world. Like other Archean terranes, it is dominated by greenstone belts and granitic plutons. Understanding the magmatic source of these rocks provides insight into crustal growth in the Archean. While the granitoids are frequently metamorphosed, they preserve certain chemical distinctions that are difficult to distinguish in the field. Some of the syn- to post-tectonic plutons are chemically enriched and termed sanukitoids (Mg# > 0.60, Ni and Cr > 100 ppm, Sr and Ba > 1000 ppm, LREE > 100X chondrites, Shirey and Hanson 1984). The genesis of sanukitoid magmas is thought to be distinct from the more common TTG suite (tonalite, trondhjemite, granodiorite) and to result from melting of the mantle wedge, metasomatized by fluids from subducted upper oceanic crust (Fig. 10; Shirey and Hanson 1984, Stern et al. 1989, Stern and Hanson 1991).

The $\delta^{18}O$ of magmatic zircons from 59 granitoids across the Superior Province (Fig. 11) shows clear bimodality of $\delta^{18}O$, in spite of restricted total range in values (Fig. 12A, King et al. 1998b). Coexisting quartz was analyzed for some samples and the same bimodality is not seen (Fig. 12B), showing that zircons are the most faithful record of magmatic $\delta^{18}O$ and that quartz can be reset by post-magmatic events (see Valley and Graham 1996). Sanukitoid zircons average $\delta^{18}O$ = 6.4±0.2‰, while the

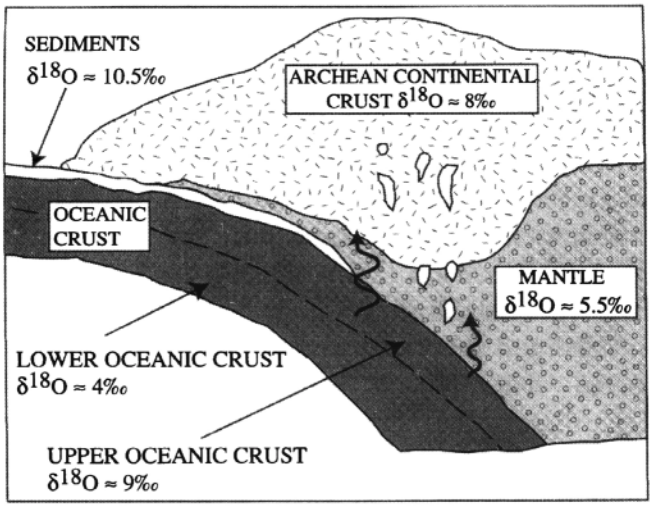

Figure 10. Schematic model for genesis of sanukitoid magmas after Stern et al. (1989). The relatively high $\delta^{18}O$ of sanukitoid magmas is inherited from high $\delta^{18}O$ fluids from the upper portions of subducted ocean crust (from King et al. 1998b).

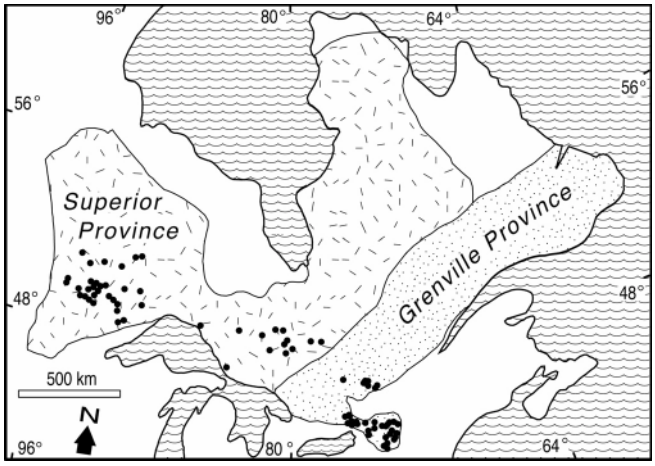

Figure 11. The Grenville and Superior Provinces of North America. Dots show zircon sample localities summarized by Peck et al. (2000). The Adirondack Mountains are a southeastern outlier of the Grenville (from Peck et al. 2000).

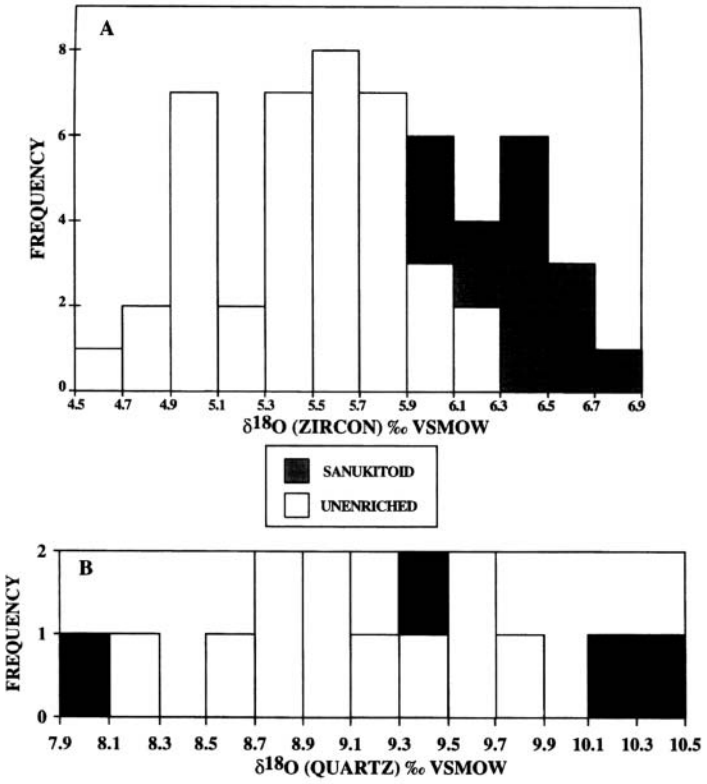

Figure 12. Histograms of $\delta^{18}O$(Zc) (A) and $\delta^{18}O$(Qt) (B) for granitoids from the Superior Province. Sanukitoid magmas are shown to be systematically higher in $\delta^{18}O$ by analysis of zircons, but this difference is not seen in analyses of quartz, which suffer variable amounts of post-magmatic exchange (from King et al. 1998b).

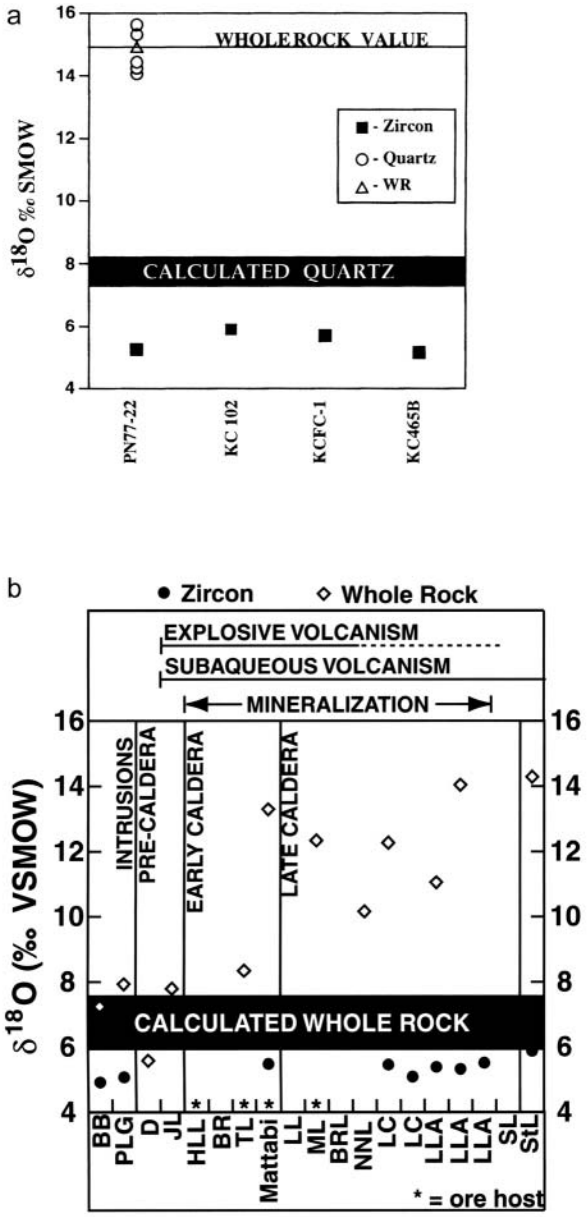

Figure 13. (a) Values of $\delta^{18}O$ for zircon, quartz and whole rock from rhyolites at the Kidd Creek Mine. "Calculated Quartz" is the $\delta^{18}O$ value in equilibrium with magmatic zircons at 900°C. Measured $\delta^{18}O(Qt)$ is ~7‰ higher than calculated, and individual quartz phenocrysts vary by up to 2‰ as the result of extreme hydrothermal alteration of quartz phenocrysts during silicification of rhyolite. Values of $\delta^{18}O(Zc)$ are identical to those in felsic volcanic rocks throughout the Superior province showing that zircons were not affected by post magmatic alteration (from King et al. 1997). (b) Values of $\delta^{18}O$ for zircons and whole rock from the Sturgeon Lake caldera complex. "Calculated whole rock" represents equilibrium at 800°C. Samples are arranged oldest to youngest (left to right). Stars indicate ore deposits. Measured whole rock $\delta^{18}O$ is elevated relative to zircons by post magmatic hydrothermal alteration (from King et al. 2000).

unenriched TTGs average 5.5±0.4‰. These values correspond to whole rock magma values of ~7 and 8‰, respectively, supporting the subduction-related model (Fig. 10).

Volcanogenic massive sulfide deposits

Kidd Creek (Ontario, 2.7 Ga) is one of the largest volcanogenic massive sulfide (VMS) Cu-Zn-Ag deposits in the world. The syngenetic origin of these ores is no longer in question, but the source and timing of high $\delta^{18}O$ values in associated rhyolites are disputed. Huston et al. (1996) and Taylor and Huston (1998) showed a correlation of $\delta^{18}O$ for quartz phenocrysts from rhyolite hosts to VMS deposits worldwide to the tonnage of zinc. These data included the footwall rhyolite at Kidd Creek. Huston et al. concluded that $\delta^{18}O(Qt)$ values are magmatic and they proposed a genetic model

correlating larger ore deposits to high-$\delta^{18}O$ S-type magmas, which formed from melting and assimilation of altered crust. More recently, Taylor and Huston (1999, p373) concluded: "In summary, the quartz phenocryst data suggest a minimum $\delta^{18}O$ value for most of the rhyolitic magmas in the Kidd Creek Volcanic Complex of 8.5 per mil."

King et al. (1997, 1998a) applied three tests to determine if the high $\delta^{18}O$ values of quartz in Kidd Creek rhyolites are magmatic or post magmatic in origin. If the phenocryst values are magmatic then: (1) quartz and zircon should preserve consistent high temperature fractionations; (2) quartz phenocrysts should have constant $\delta^{18}O$ at hand sample scale; and (3) individual quartz phenocrysts should be homogeneous in $\delta^{18}O$ or show minor magmatic growth zoning. These tests were guided by careful examination of textures in thin section by optical and cathodoluminescent microscopy (CL). Figure 13a shows $\delta^{18}O$ of zircons that had previously been dated by U-Pb. Eleven different magnetic splits from four rocks all have the same $\delta^{18}O(Zc) = 5.4\pm0.3‰$, which is indistinguishable from other TTG zircons in the same province (5.5±0.4‰, Fig. 12A) and is the mantle value that would be expected in a primitive I-type felsic magma. Such constant mantle-like values are found in zircons from all plutonic and volcanic rocks in the Superior Province with the exception of the sanukitoids (Fig. 14) and these values provide a boundary condition for evaluating post magmatic processes. Magmatic quartz in equilibrium with these zircons would have $\delta^{18}O \approx 7.5\text{-}8.0‰$ and whole rock values for the magma of 6.5 to 7.0‰ (Fig. 13a; $\Delta^{18}O(Qt\text{-}Zc) = 1.92$ at 900°C, Valley et al. 2003). All 27 of the measured quartz and all but a few of the 377 whole rock $\delta^{18}O$ values at Kidd Creek (Taylor and Huston 1999) are higher than these magmatic values indicating that quartz and rock matrix have been elevated in $\delta^{18}O$ by processes after the crystallization of zircon. Figure 13a shows the values of five individual quartz phenocrysts from one sample with a range of $\delta^{18}O = 14.2$ to 16.1. Ion microprobe analysis of single quartz crystals from this sample further shows intracrystalline variability of up to 4‰, which correlates to high $\delta^{18}O$ veins and crack-healing at the μm-scale, documenting the post-magmatic process whereby quartz values are elevated. Thus, none of the tests support the preservation of magmatic $\delta^{18}O$ values in quartz from these rhyolites. Recognition that magmatic values are 1 to 4‰ lower than previously thought has profound implications for the thermal and fluid history of the deposit. Oxygen isotope thermometry and calculation of fluid composition should not employ isotopically heterogeneous quartz unless an appropriate microanalytical technique is available. King et al. (1997, 1998a) conclude that zircons are the best record of magmatic $\delta^{18}O$ at Kidd Creek, that quartz and whole rock were elevated in $\delta^{18}O$ by post magmatic hydrothermal alteration as originally proposed by Beatty et al. (1988), and that the correlation seen by Huston et al. (1996) could arise if the specific characteristics of hydrothermal systems (size, source, duration, fracturing, temperature) create larger ore deposits and more intensely altered quartz.

The Sturgeon Lake caldera complex (Ontario, 2.7 Ga) is host to several VMS deposits. As at Kidd Creek, igneous zircons average $\delta^{18}O = 5.4\pm0.3‰$ (n = 12), but quartz and whole rock compositions have been elevated throughout the 18 Myr sequence by post magmatic hydrothermal alteration (Fig. 13b; King et al. 2000). The magnitude of $^{18}O/^{16}O$ enrichment is moderate, 1-2‰, in the pre- and early caldera units, but becomes greater, 4-7‰, in late and post-caldera rocks above the Mattabi unit, supporting the model that impermeable volcanic layers control the size and location of hydrothermal systems.

Hadean detrital zircons

Events of the first 500 Myr of Earth history are inherently uncertain because no known rocks have been preserved. The only solid evidence before 4.0 Ga comes from rare detrital and xenocrystic zircons, the oldest of which is 4.4 Ga (Wilde et al. 2001). Values of $\delta^{18}O$, measured in single zircons by ion microprobe (4.4-3.3 Ga; Fig. 15), show the same range in values, 5-8‰, as seen by conventional analysis, throughout the Archean (3.5-2.6 Ga; Fig. 16). Values of $\delta^{18}O(Zc)$ that are higher than 6.5‰ are above the mantle-derived value and suggest a history with surface alteration of protolith by liquid water at low temperatures to elevate $\delta^{18}O$, burial, melting to form high $\delta^{18}O$ felsic

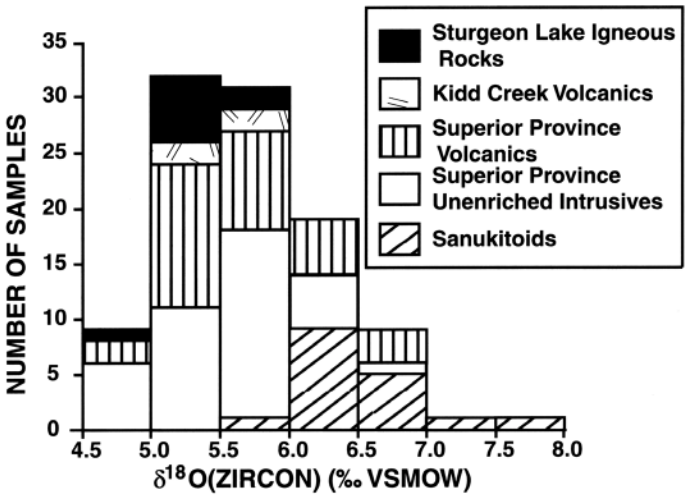

Figure 14. Histogram of $\delta^{18}O$ for magmatic zircons from volcanic and plutonic rocks of the Superior Province (from King et al. 2000).

magma, and then crystallization of high $\delta^{18}O$ zircon (Peck et al. 2001, Mojzsis et al. 2001, Valley et al. 2002). Other on-going measurements on these tiny (100-200 μm) time capsules include CL and BSE imaging, REE analysis, identification of μm-scale inclusions, nano-XANES (i.e., X-ray photo-electron emission spectro-microscopy; Gilbert et al. 2003), and radiogenic isotope geochemistry (Cavosie et al. 2002). There is no primitive reservoir in the mantle or in meteorites that can explain the geochemistry of the higher $\delta^{18}O$ zircons. The best interpretation of existing data is that the Earth cooled quickly after accretion, and formation of the core and the Moon, that liquid water was stable on the surface as early as 4.4 Ga, and that differentiated continental-type crust was starting to form. If the Earth's hydrosphere was in place by this time, surface temperatures are suggested below 200°C, low enough to precipitate oceans with possible biologic implications. The rapid cooling required by this hypothesis provides a boundary condition for models of insulation by the earliest atmosphere and for the energy input from Earth bombardment by meteorites (Fig. 17; Valley et al. 2002). Further samples are being sought to test these hypotheses.

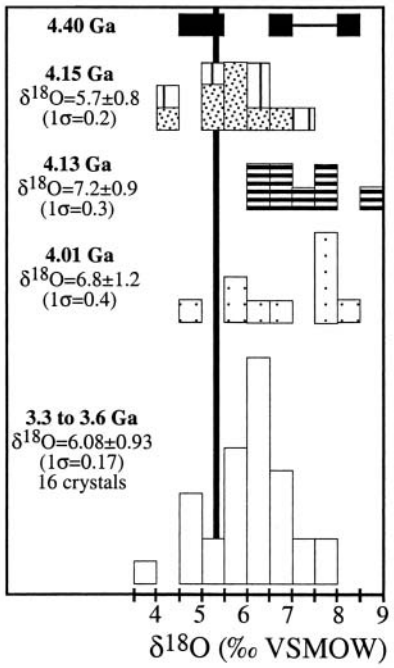

Figure 15. Compilation of $\delta^{18}O$ analyses by ion microprobe for detrital zircons from Jack Hills, Western Australia. All age groups except 4.15 Ga are elevated in $\delta^{18}O$ with respect to mantle values (solid line) or ion microprobe analyses of a homogeneous zircon standard (from Peck et al. 2002).

Mid-Proterozoic

Anorthosite suite. Magmatic zircons from the Grenville Province have been studied from:

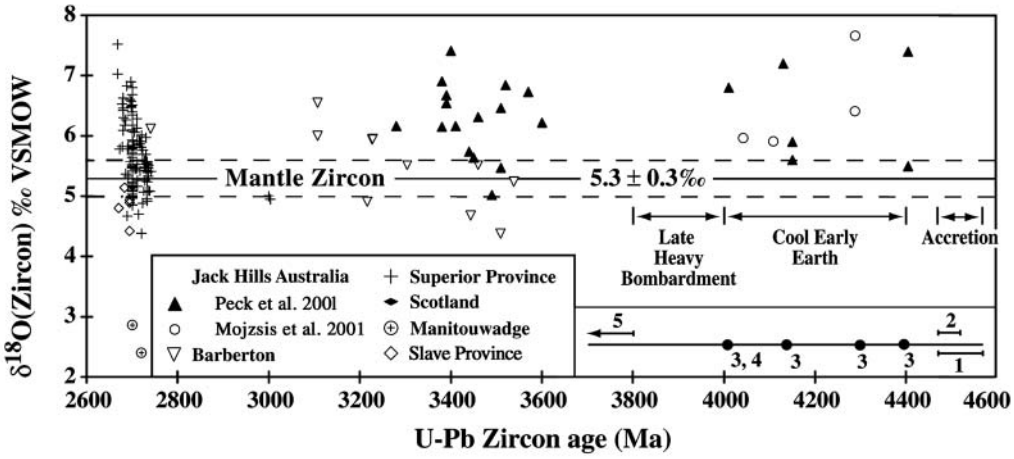

Figure 16. Crystallization age (U-Pb) and $\delta^{18}O$ for Archean magmatic zircons. A majority of magmas were primitive in $\delta^{18}O$ similar to the mantle today ("mantle zircon"), but some zircons are elevated as high as 7.5‰ due to melting of protoliths that were altered at low temperature by liquid water near the surface of the Earth. The timeline, lower right, shows: 1. accretion of Earth; 2. formation of Moon and Earth's core; 3. evidence for liquid water; 4. Acasta gneiss; 5. Isua metasediments (from Valley et al. 2002).

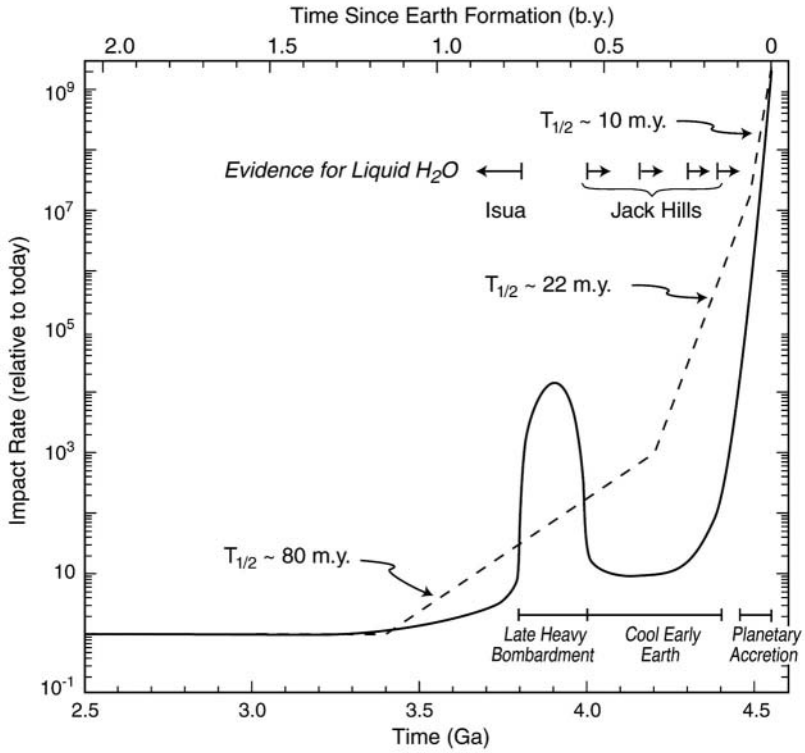

Figure 17. Estimates of meteorite flux for the first 2 Gyr of Earth history based on two hypotheses: exponential decay of impact rate (dashes) and cool early Earth / late heavy bombardment (solid curve). The hypothesis of a cool early Earth suggests that impact rate dropped precipitously by 4.4 Ga, consistent with relatively cool conditions and liquid water oceans (from Valley et al. 2002).

massif-type anorthosites and associated granitic rocks (AMCG suite), from granitic rocks of other age (non-AMCG), and from quartzites (detrital zircons) (Chiarenzelli and McLelland 1993, Valley et al. 1994, Peck 2000, Peck et al. 2003a,b; Clechenko et al. 2002). The intrusion of AMCG plutons as high $\delta^{18}O$ magmas is discussed above (Assimilation vs. Fractional Crystallization) and demonstrates a major crustal component in both the anorthosite and enclosing contemporaneous granitic rocks. (Fig. 18; open circles).

Zircons from monzosyenite associated with the Laramie anorthosite (Wyoming) have a uniform $\delta^{18}O = 7.4\pm0.2‰$ (O'Connor and Morrison 1999). In contrast to the Grenville anorthosites, this value is too high for magmatic equilibration with the associated anorthosite, suggesting a major crustal component to the granitic magmas and ruling out closed system fractionation from the same parent magma as anorthosite. One zircon from pegmatite associated with the San Gabriel anorthosite (Pacoima Canyon, California) has a mantle-like value of 5.69‰ warranting further study (Valley, unpublished).

Grenville terrane boundaries. The Carthage-Colton Mylonite Zone and the Maberly Shear Zone are major terrane boundaries in the Grenville Province, separating the Adirondack Highlands, the Frontenac terrane, and the Sharbot Lake domain (Fig. 19). The Carthage-Colton and its continuation in Quebec, the Labelle Shear zone, extend over 400 km separating terranes with distinct lithology, and timing and intensity of metamorphism. Competing views interpret this boundary as the site of terrane docking during the Elzevirian Orogeny (ca. 1.35-1.18 Ga) or as a post metamorphic normal fault down-dropping amphibolite facies rocks of the NW Adirondacks to become adjacent to granulites in the Adirondack Highlands. Metamorphosed plutonic rocks of the ~1.15 Ga AMCG suite occur on both sides of this boundary suggesting that the terranes were juxtaposed by ~1.18 Ga (McLelland et al. 1996).

The high $\delta^{18}O$ of Adirondack and Frontenac orthogneisses has long been recognized (Taylor 1969, Shieh 1985, Morrison and Valley 1988). While metamorphic fluid-hosted origins for this anomaly have been proposed, the high $\delta^{18}O$ values in magmatic zircons from all phases of the AMCG suite (Valley et al. 1994, Clechenko et al. 2002, Peck et al. 2003a,b), preclude a post-metamorphic origin and demonstrates that these were high $\delta^{18}O$ magmas, as originally proposed by Valley and O'Neil (1984).

Figure 19 shows values of $\delta^{18}O$(Zc) from AMCG ortho-gneisses across the Adiron-dacks and Frontenac terrane (Peck et al. 2003b). Values of $\delta^{18}O$ are projected onto a NW-SE traverse. Remarkably homogeneous, yet elevated values of 8.2±0.6‰ are seen throughout the Adirondack Highlands. These high magmatic $\delta^{18}O$ values include granitic rocks that are 2-3‰ enriched in $^{18}O/^{16}O$ relative to primitive mantle-derived magmas. In con-

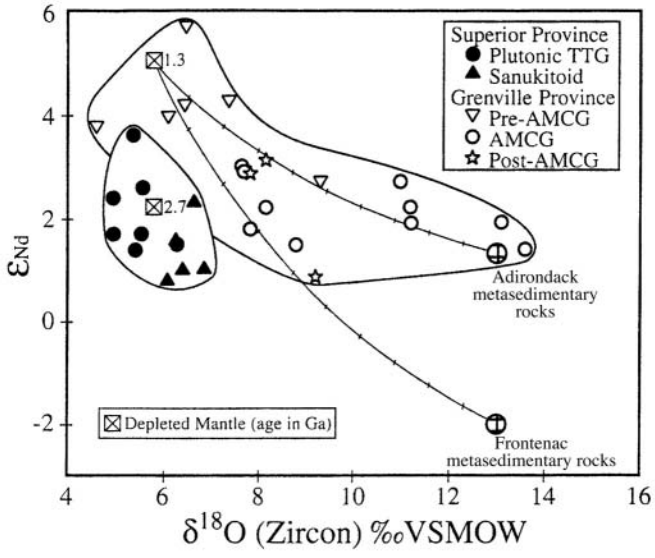

Figure 18. Values of whole rock ε_{Nd} vs. $\delta^{18}O$(Zc). Superior Province samples show little variability and cluster around the value for depleted mantle at 2.7 Ga. Samples from AMCG and post-AMCG plutons in the Grenville fall along mixing trends with metasediment. Pre-AMCG magmas were more mantle-like (from Peck et al. 2000).

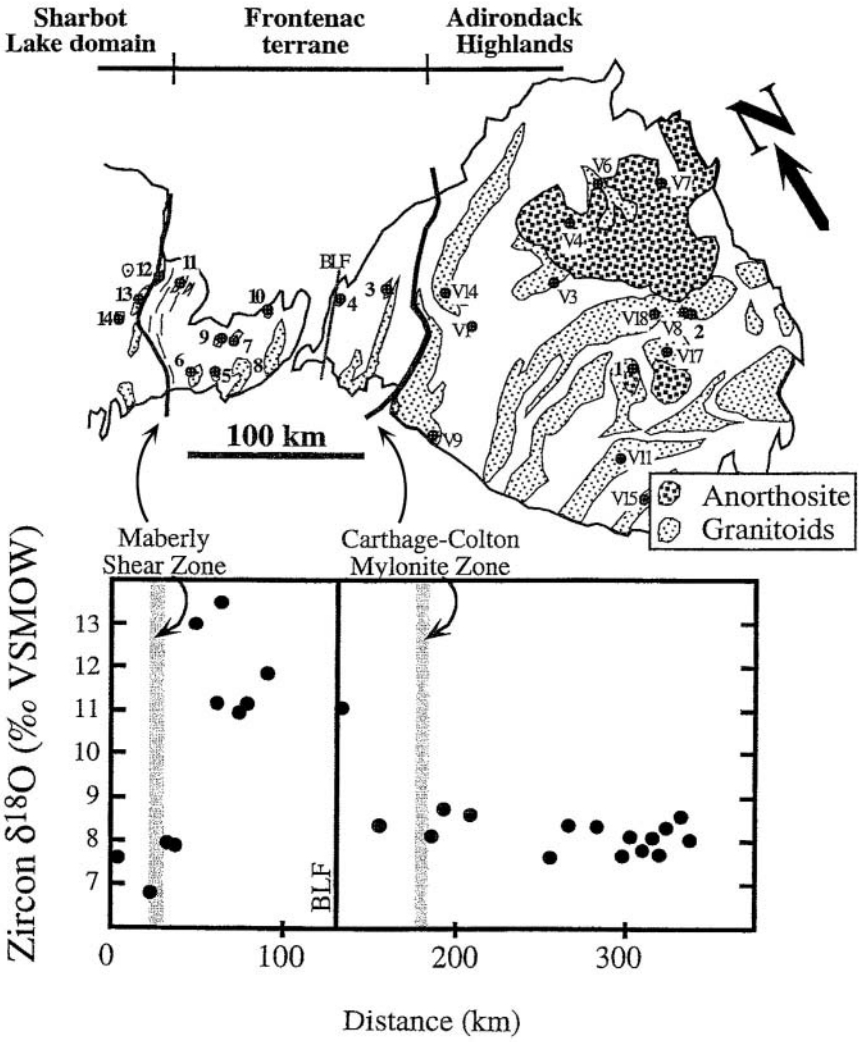

Figure 19. Values of $\delta^{18}O$(Zc) and sample locations from AMCG (anorthosite-suite) plutons (1180-1130 Ma) of the Adirondack Highlands and Frontenac terrane of the Grenville Province. The Carthage-Colton mylonite zone is a major shear zone separating the two terranes and extending over 400 km north into Quebec. Values of $\delta^{18}O$ are 2-3‰ higher than primitive mantle magmas in the Adirondacks, but jump to over 10‰ in the Frontenac revealing that high $\delta^{18}O$ sediments occur at depth. Subduction of supra-crustal rocks is proposed during the Elzevirian Orogeny followed by melting during AMCG plutonism (from Peck et al. 2003b).

trast, the zircons of the Frontenac terrane are higher still and more variable at 11.8±1.0‰. These values include the highest $\delta^{18}O$ yet measured in magmatic zircon (13.5‰) and represent granitic plutons with magmatic whole rock values up to 15‰. Farther to the NW, across the Maberly Shear Zone, this high $\delta^{18}O$ anomaly is not seen. While elevated $\delta^{18}O$ values extend from the Adirondack Highlands north to the Morin anorthosite (Peck and Valley 2000), the unusually high Frontenac values have not been found farther north along strike of the Frontenac Terrane. The $\delta^{18}O$ of Frontenac AMCG magmas cannot be caused by exchange with country rocks at the present levels of exposure (Peck et al. 2003b) and thus the zircon data document the otherwise undetected existence of unusually high $\delta^{18}O$ source rocks at depth. Consistent with the tectonic model of McLelland et al. (1996) and Wasteneys et al. (1999), Peck et al. (2003b) hypothesize subduction of high $\delta^{18}O$ sediments

and altered ocean crust during the Elzevirian Orogeny at ~1.2 Ga followed by melting and AMCG plutonism at 1.18-1.13 Ga. The surprising bimodality of $\delta^{18}O(Zc)$ across the Carthage-Colton mylonite for rocks of the same suite indicates that the deep crust under the Frontenac terrane is unique and suggests either that the Frontenac was the continental margin to Elzevirian subduction or that the two terranes were separated at that time.

Finnish Svecofennian granitoids. Values of $\delta^{18}O(Zc)$ from 1.88-1.87 Ga post-kinematic, and 1.65-1.54 Ga anorogenic rapikivi, magmatism in Finland provide information on crustal evolution during the Svecofennian Orogeny (Elliott et al. 2001). Undeformed 1.88-1.87 Ga granitoids are relatively constant at $\delta^{18}O(Zc) = 6.22\pm0.48‰$, while three plutons adjacent to supracrustal lithologies are higher, 7.70±0.09‰. Values in 1.65-1.54 Ga plutons vary south to north across a probable terrane boundary and correlate with Nd isotopes; in the south $\delta^{18}O(Zc) = 6.14\pm0.07‰$ and $\varepsilon_{Nd} = -0.9$ to +0.7, while in the north $\delta^{18}O(Zc) = 7.95\pm0.68‰$ and $\varepsilon_{Nd} = 1.5$ to 3.0. Interestingly, the more evolved, higher $\delta^{18}O$ correlates to ε_{Nd} that is slightly more primitive.

CRUSTAL GROWTH AND MATURATION

The oxygen isotope geochemistry of crust-derived magmas reflects the long term mixing of mantle derived melts and the crust. Recycled sediments and other supra-crustal materials most commonly have $\delta^{18}O$ higher than the mantle due to low temperature processes, but a lower $\delta^{18}O$ is also possible. Through time, the crust has matured as granitoids with mildly elevated $\delta^{18}O$ are also recycled creating larger $^{18}O/^{16}O$ enrichment. Analyses of $\delta^{18}O$ in zircons that have been dated provide a record of the growth and maturation of the crust.

Superior vs. Grenville province

Peck et al. (2000) compared Archean zircons (3.0-2.7 Ga) from the Superior Province (King et al. 1997, 1998b; King 1997) to Proterozoic zircons (1.3-1.0 Ga) from the Grenville Province (Valley et al. 1994, Peck 2000). Samples are from a 2000 km traverse across the Grenville Front (Fig. 11). A pronounced bimodality in $\delta^{18}O$ exists. Magmatic zircons from the Superior Province are relatively constant and mantle-like with average $\delta^{18}O = 5.7\pm0.6‰$ (1sd). In contrast, magmatic zircons from the Grenville are on average 2.5‰ higher and much more variable in $\delta^{18}O = 8.2\pm1.7‰$ (Fig. 20). Peck et al. (2000) conclude that the primitive values in the Superior Province result from relatively low amounts of crustal burial, subduction and recycling in the Archean, and from the relatively low and mantle-like $\delta^{18}O$ of Archean sediments that were available for recycling. In contrast, maturation of the crust by mid-Proterozoic time provided large amounts of higher $\delta^{18}O$ supracrustal material and active subduction promoted more vigorous recycling.

The rapid recycling of the

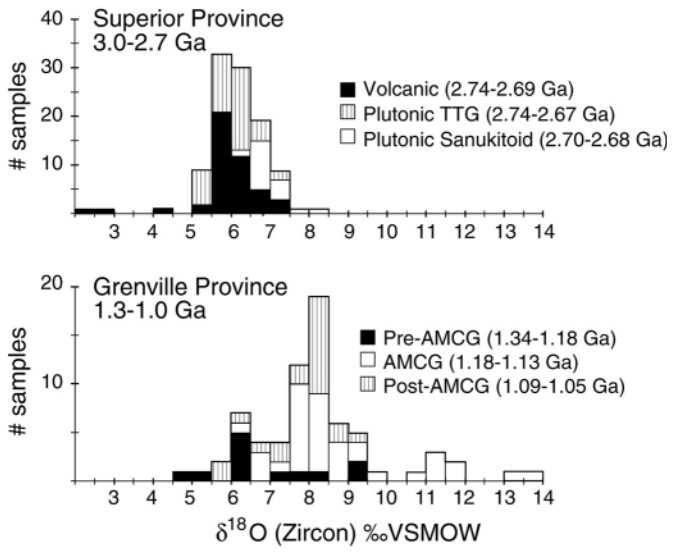

Figure 20. Values of $\delta^{18}O$ for magmatic zircons from the Grenville (1.3-1.0 Ga) and Superior Provinces (3.0-2.7 Ga). The Archean Superior Province samples have consistently low and primitive $\delta^{18}O(Zc) = 5.7\pm0.6‰$. The Proterozoic Grenville samples are more evolved with variable and high $\delta^{18}O(Zc) = 8.2\pm1.7‰$. (from Peck et al. 2000).

Grenville crust is dramatically demonstrated by the oxygen isotope ratios (Fig. 20), but is not well documented by radiogenic isotope studies. Peck et al. (2000) review published radiogenic isotope data and point out that the anorthosite-suite (AMCG) rocks, which comprise 30% of the Grenville, appear to be "juvenile Middle Proterozoic additions to only slightly older (<1.4 Ga) crust, suggesting a relatively short history, and likely derivation from the mantle." Figure 18 shows whole rock ε_{Nd} vs. $\delta^{18}O(Zc)$. The ε_{Nd} values for the Grenville at 1.3 Ga are positive with a restricted range of <5 ε_{Nd} units showing that the recycled high $\delta^{18}O$ material was relatively juvenile, but radiogenic isotopes do not distinguish among Middle Proterozoic sources that are magmatic vs. sedimentary. In contrast to the Archean, where no recycling is evident, the Grenville data show a negative correlation of $\delta^{18}O(Zc)$ and ε_{Nd} (Fig. 18). Thus, the high $\delta^{18}O$ values show that material recycled into the source regions of AMCG magmas had a relatively short history of low temperature alteration rapidly followed by subduction or burial, and melting.

Evolution of magmatic $\delta^{18}O$ through time

Magmatic zircons of known age (4.4 Ga to 0.2 Ma) have been analyzed by laser fluorination at the University of Wisconsin from over 600 rocks worldwide to test the generality of $\delta^{18}O$ differences between the Grenville and Superior Provinces (Fig. 21). U-Pb ages were determined previously for most samples by thermal ionization mass-spectrometry. The Jack Hills detrital zircons were analyzed *in situ* by ion microprobe.

The range and variability of $\delta^{18}O$ in the Archean is subdued. Values at ~2.7 Ga are largely from the Superior Province with most zircons in high temperature equilibrium with the mantle and a tail to higher values (Figs. 14, 16, 20a). No magmatic zircons have been analyzed in the Archean with $\delta^{18}O > 8‰$. Similar values come from the Lewisian (2.7 Ga), Slave Province (2.7 Ga), and Barberton (2.7-3.5 Ga, Kamo and Davis 1994). The Jack Hills zircons (4.4-3.1 Ga) are indistinguishable within uncertainty.

Values of $\delta^{18}O(Zc)$ are significantly more variable in the Proterozoic and Phanerozoic. Many values are above 8‰, suggesting that magmas with whole rock $\delta^{18}O > 9$-10‰ became common after 2.5 Ga and were derived from high $\delta^{18}O$ crustal rocks. However, values of $\delta^{18}O(Zc) > 10‰$ are not common. In the Grenville, they come from a relatively small group of plutons that were intensely studied (Shieh 1985, Peck et al. 2003b). Likewise samples with $\delta^{18}O < 5‰$ are over represented due to studies of low

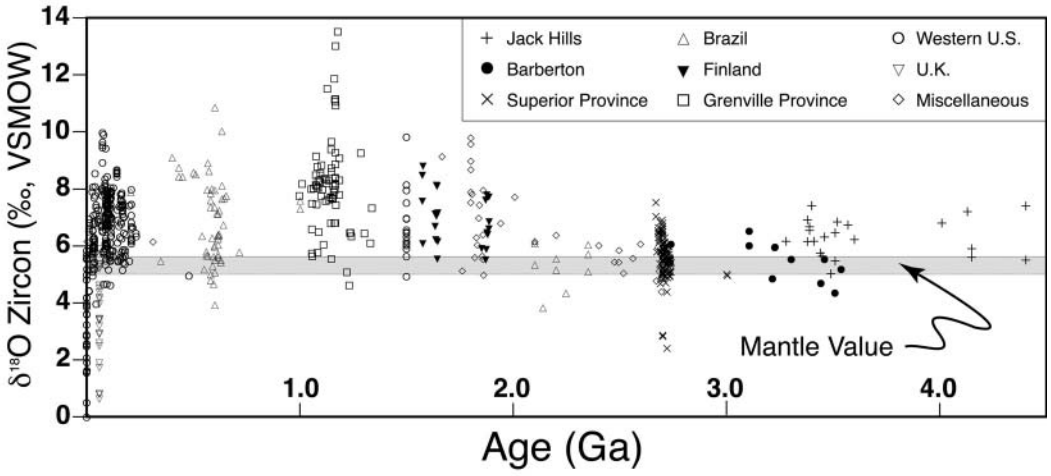

Figure 21. Compilation of $\delta^{18}O(Zc)$ vs. age for over 600 samples analyzed at the University of Wisconsin. Samples range in age from 4.4 Ga to 0.2 Ma and come from many terranes on seven continents. A remarkable uniformity is seen in the Archean, values cluster near the mantle ($\delta^{18}O(Zc) = 5.3\pm0.3‰$) with some values as high as 7.5‰ due to recycling of supracrustal material. High $\delta^{18}O$, above 8‰ does not become common until after 2 Ga, reflecting recycling of high $\delta^{18}O$ sediment. This change may be due to the onset of subduction, the evolution of mature sediments, or changes in the Earth's atmosphere near the end of the Archean.

$\delta^{18}O$ granites from the British Tertiary Igneous Province and low $\delta^{18}O$ rhyolites from Yellowstone.

The nature of the Archean-Proterozoic $\delta^{18}O(Zc)$ transition is not yet known due to the relatively small data set between 2.5 and 2.0 Ga. Perhaps this is a sharp transition at the end of the Archean or at some date within the next 500 m.y., or perhaps it was a gradual change. Either way, it is expected that many samples would be mantle-like and more analysis will be necessary to determine if higher $\delta^{18}O$ magmas existed at this time interval. Possible causes for this change include: changes in the composition and abundance of sediments available for recycling due to increased sedimentary environments at the end of the Archean; the onset or acceleration of subduction at the end of the Archean (if one rejects Archean subduction); or differences in weathering as the atmosphere became more oxygen rich at ~2.2 Ga.

ULTRA-HIGH PRESSURE ECLOGITES, DABIE AND SULU

The Dabie-Sulu orogenic belt separates rocks of the Sino-Korean Plate from the Yangtze Plate in China. Movement along the Tan-Lu fault has separated Dabie Shan and Sulu by 500 km, but they are linked by unique petrologic and geochemical characteristics. Eclogite facies metamorphism produced rare ultra high pressure (UHP) mineral assemblages including coesite and diamond in the Triassic (245-210 Ma) and many UHP rocks are depleted in $^{18}O/^{16}O$ demarking an original area extending over 100 km, one of the major hydrothermally altered terranes on Earth. Values of $\delta^{18}O$(garnet) and $\delta^{18}O$(Qt) as low as –10‰ document exchange with heated meteoric waters, but the age of alteration has been uncertain.

Rumble et al. (2002) found values of $\delta^{18}O(Zc)$ = –0.2 to –7.4‰ from granites near Qinglongshan in Sulu and used *in situ* ion microprobe analysis to date zircon cores to 754-684 Ma. Air abrasion and laser fluorination of zircons revealed no zoning in $\delta^{18}O$ (cores vs. whole grains), showing that cores are low in $\delta^{18}O$ and thus that the low $\delta^{18}O$ anomaly was acquired almost 500 m.y. before UHP metamorphism. The coincidence of magmatism, extremely low $\delta^{18}O$ meteoric water, and Neoproterozoic continental glaciation (Nantuo tillite, ~800-700 Ma) has led to the proposal that granites intruded in proximity to glacial ice. Presumably, the granites were melted from, and contaminated by, low $\delta^{18}O$ hydrothermally altered country rocks as has been documented at Yellowstone (see, Bindeman and Valley 2001). Paleolatitudes of 29 to 43° are estimated for Dabie supporting the hypothesis that these conditions were part of a worldwide "Snowball Earth" event (Hoffman et al. 1998, Rumble et al. 2002). These conclusions are strengthened by Zheng et al. (2003) who analyzed 112 zircon samples from eclogites and granitic orthogneisses throughout Dabie and Sulu with values as low as –10‰, which are the lowest $\delta^{18}O$ zircons known. Values range from –4.6 to +8.9‰ in Dabie and –10.3 to +5.6‰ in Sulu.

In contrast to the metamorphosed granites, Wei and Valley (unpublished) analyzed zircons from 45 samples from 15 younger unmetamorphosed granitic plutons and associated country rocks at Dabie. Values for granite range from –1.63 to 6.08‰ with an average of 5.01±0.95‰ (n = 38). These values for unmetamorphosed granites are similar to other Mesozoic and Tertiary granites in eastern China and show that the ultra-low $\delta^{18}O$ anomaly at Dabie and Sulu is restricted to rocks that predated the ultra high-pressure metamorphism.

FELSIC VOLCANISM, WESTERN UNITED STATES

Three volcanic centers from the western U.S. have produced large volume rhyolitic eruptions (≥650 km^3) and calderas, and have been studied in detail: Yellowstone, Timber Mountain/ Oasis Valley, and Long Valley. The analysis of $\delta^{18}O$ in magmatic zircons has provided information not previously available regarding the remelting of wall rocks, and the duration of magmas and magma chambers.

Low $\delta^{18}O$-rhyolites, Yellowstone

The Yellowstone Plateau is the present terminus of an NE-migrating hotspot that has caused one of the largest centers of rhyolitic magmatism on Earth. Three massive (100-2500 km^3), caldera-

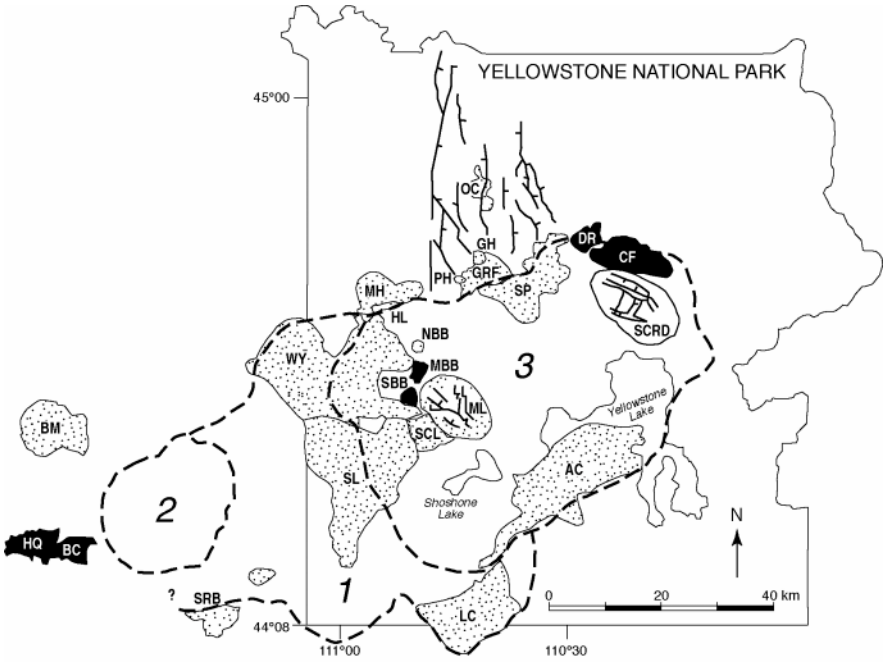

Figure 22. Yellowstone Plateau, showing the positions of major calderas: 1. Big Bend caldera, Huckleberry Ridge Tuff, 2.0 Ma, 2500 km^3; 2. Henry Forks caldera, Mesa Falls Tuff, 1.3 Ma, 300 km^3; 3. Yellowstone caldera, Lava Creek Tuff, 0.6 Ma, 1000 km^3. For sources of mapping, see Christiansen (2000). Flows in black are low $\delta^{18}O$ rhyolites. The Mallard Lake (ML) and Sour Creek (SCRD) resurgent domes are within Yellowstone caldera (from Bindeman and Valley 2001).

forming, and numerous smaller, lavas and tuffs (Fig. 22) have erupted over the past 2 million years, covering most of the western United States (Christiansen 2000). Early oxygen isotope analyses of quartz found that low $\delta^{18}O$ rhyolites follow each of the climactic eruptions (Fig. 23a; Lipman and Friedman 1975, Hildreth et al. 1984). The low $\delta^{18}O$ post-caldera rhyolites are relatively small (<50 km^3) and are themselves followed by a return to normal magmatic values.

The genesis of low $\delta^{18}O$ rhyolites at Yellowstone and the implications for explosive volcanism have been vigorously debated. Lipman and Friedman (1975) and Hildreth et al. (1984) proposed that low $\delta^{18}O$ meteoric waters coursed down the caldera-forming fracture system and interacted directly with underlying bodies of magma. Taylor and Sheppard (1986) argued that significant interaction of liquid water with a magma chamber was impossible on physical grounds. Instead, they proposed the assimilation of hydrothermally altered, low $\delta^{18}O$ wall rock. Likewise, Bacon et al. (1989) proposed that partial melting of wall rock caused low $\delta^{18}O$ magmas at Crater Lake.

Bindeman and Valley (2000a, 2001) separated and analyzed zircons and coexisting minerals from 25 lavas and tuffs at Yellowstone (Fig. 23b). The fractionation between quartz and zircon is equilibrated and normal (~2.1‰) for most magmas. In contrast, extreme disequilibrium was found among zircon and other minerals in low $\delta^{18}O$ rhyolites erupted after the two largest caldera-forming eruptions (Fig. 23b; Huckleberry Ridge at 2 Ma and Lava Creek at 0.6 Ma). This is evident from values of Δ(Qt-Zc) that are too small for any magmatic temperature (Fig. 23d), or reversed, and from oxygen isotope zonation within zircons (Figs. 23c, 24). Zoning within single zircons shows rims up to 5‰ lower than cores based on: analysis of early-formed large zircons vs. late-formed smaller zircons; air abrasion of large zircons and comparison of cores to whole crystals; and ion microprobe analysis of cores and the outer 3 μm of rims (Fig. 24).

The discovery of isotopically zoned zircons at Yellowstone supports a revised model for the genesis of post-caldera magmas and low $\delta^{18}O$ rhyolites (Bindeman and Valley 2000a, 2001). Hy-

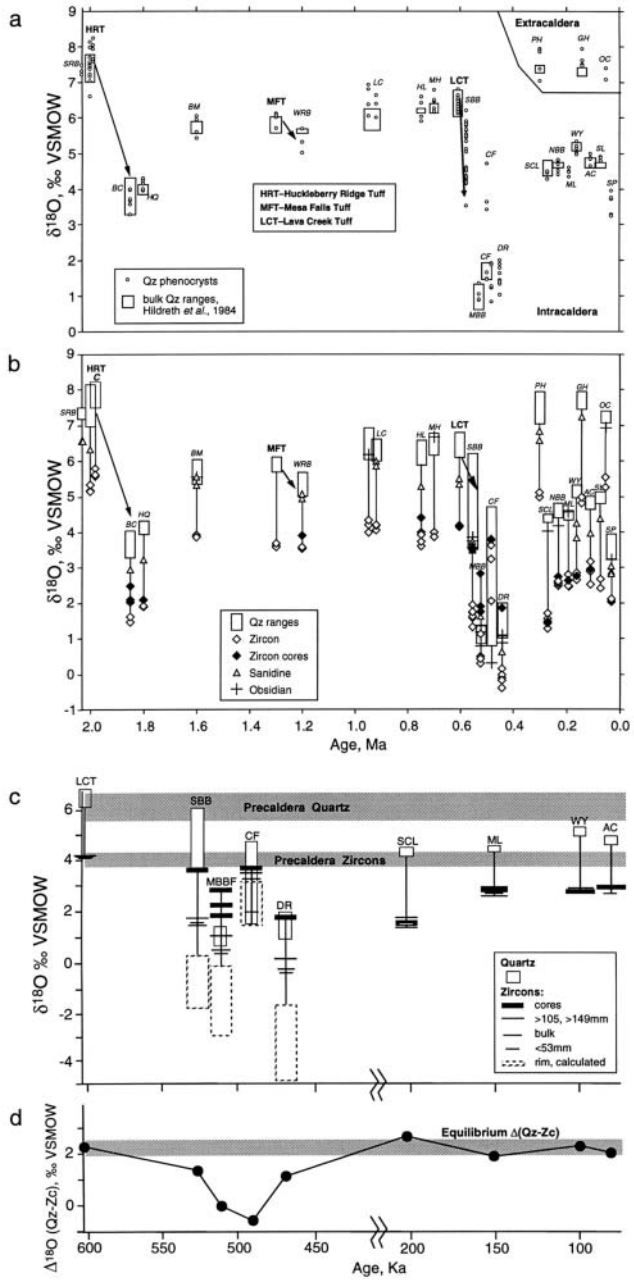

Figure 23. Evolution of $\delta^{18}O$ in Yellowstone magmas. Caldera-forming eruptions are Huckleberry Ridge Tuff (HRT), Mesa Falls Tuff (MFT), and Lava Creek Tuff (LCT). (a) Individual quartz phenocrysts and bulk quartz. (b) Zircon, sanidine, and obsidian. Air-abraded zircon cores are filled diamonds. (c) Post LCT intra-caldera lava flows. The range of individual quartz phenocrysts are shown in boxes. Zircons are plotted by crystal size. (d) $\Delta^{18}O$(Qt-Zc) for LCT and post-LCT lavas. The equilibrium value of Δ(Qt-Zc) is 1.9-2.3‰ at 800-900°C. Note that only low $\delta^{18}O$ rhyolites have quartz and zircon that are not equilibrated (from Bindeman and Valley 2000a, 2001).

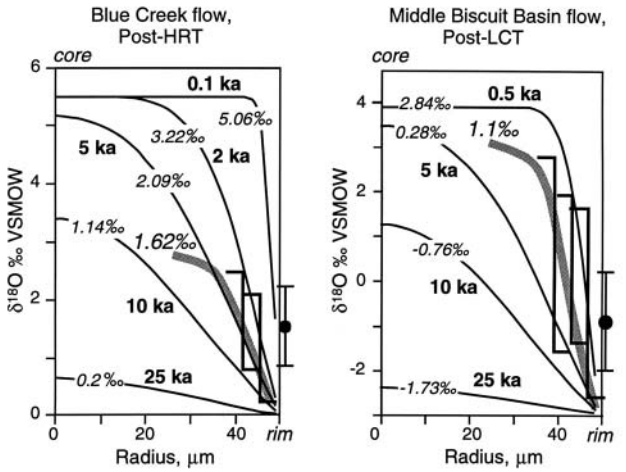

Figure 24. Zoning profiles for $\delta^{18}O$ in 50 μm radius zircons from Blue Creek and Middle Biscuit Basin flows, Yellowstone, based on: successive air abrasions and ion microprobe analysis of crystal growth faces (filled dots). The top of each bracket is the $\delta^{18}O$ of zircon cores after abrasion and the bottom of each bracket is the calculated $\delta^{18}O$ of removed rims. The radius at each step is calculated by weight. Thin curves are labeled with the bulk $\delta^{18}O$ of the grain (**bold** = measured; *italic* = estimated) and calculated using the "wet" diffusion rate (Watson and Cherniak 1997). The residence time (kyr) necessary to create each profile by diffusion between a higher $\delta^{18}O$ zircon xenocryst and a low $\delta^{18}O$ melt is shown (from Bindeman and Valley 2001).

drothermal alteration by heated meteoric waters lowers $\delta^{18}O$(WR) of rocks overlying the magma chamber, but refractory zircons and some quartz phenocrysts retain magmatic $\delta^{18}O$ (~4‰; Fig. 25,I). After climactic eruption, the roof drops to contact hot magmas remaining in the magma chamber (Fig. 25,II). Melting of the down-dropped roof zone forms magma, which is low in $\delta^{18}O$(WR), but has unaffected higher $\delta^{18}O$ zircons as xenocrysts. The eruption of these localized, small volume melts produces intra-caldera low $\delta^{18}O$ rhyolites (Fig. 25,III).

One of the implications of this model is that zoned zircons are xenocrysts from earlier rhyolites. This prediction has been verified by ion microprobe dating of post Lava Creek Tuff zircons (<0.65 Ma), which show that many zircon cores are inherited from earlier magmas (2.4 to 0.7 Ma; Bindeman et al. 2001a).

The failure of the magmatic system to achieve oxygen isotope equilibration with zircon cores provides information on the longevity of the post caldera magmas. The measured zonation profiles and low $\delta^{18}O$ rims have formed by either overgrowth of new magmatic zircon or by diffusion (Watson 1996, Watson and Cherniak 1997, Peck et al. 2003a). Bindeman and Valley (2001) estimate that if the profiles shown in Figure 24 formed by diffusion, it would take 500-10,000 years (time varies with choice of diffusion coefficient and crystal size).

Timber Mountain / Oasis Valley Caldera Complex

The SW Nevada Volcanic field includes four major caldera forming ash-flow sheets of the Timber Mountain / Oasis Valley caldera complex: Topopah Springs Tuff, >1200 km^3, 12.8 Ma; Tiva Canyon Tuff, 1000 km^3, 12.7 Ma; Rainier Mesa Tuff, 900 km^3, 11.6 Ma; and Ammonia Tanks Tuff, 1200 km^3, 11.45 Ma. Each tuff erupted an early, more voluminous rhyolite and later latite. Latites are characterized by higher values of: magmatic temperature, crystal content, and Zr, Sr, and REE content. Latites are lower in magmatic $\delta^{18}O$(WR) as calculated from $\delta^{18}O$ of phenocrysts and equilibrium fractionations. Figure 26 shows that the tuffs erupted in pairs separated by ~0.1 Myr and that the second tuff in each pair is depleted in $^{18}O/^{16}O$ by 1-2.5‰ (Bindeman and Valley 2000b, 2003). The low $\delta^{18}O$ tuffs and lavas contain zircons that are zoned by approximately 2‰ with higher $\delta^{18}O$ cores being recycled xenocrysts from melting of earlier tuffs.

These trends are similar to those observed at Yellowstone with the major difference that the volume of low $\delta^{18}O$ rhyolites is much larger and the depletions are smaller. It is likely that the four climactic eruptions expelled most of the magma from each magma chamber and that each new felsic magma formed by melting of shallow crust, heated by intrusion of mafic magma. Thus the oxygen

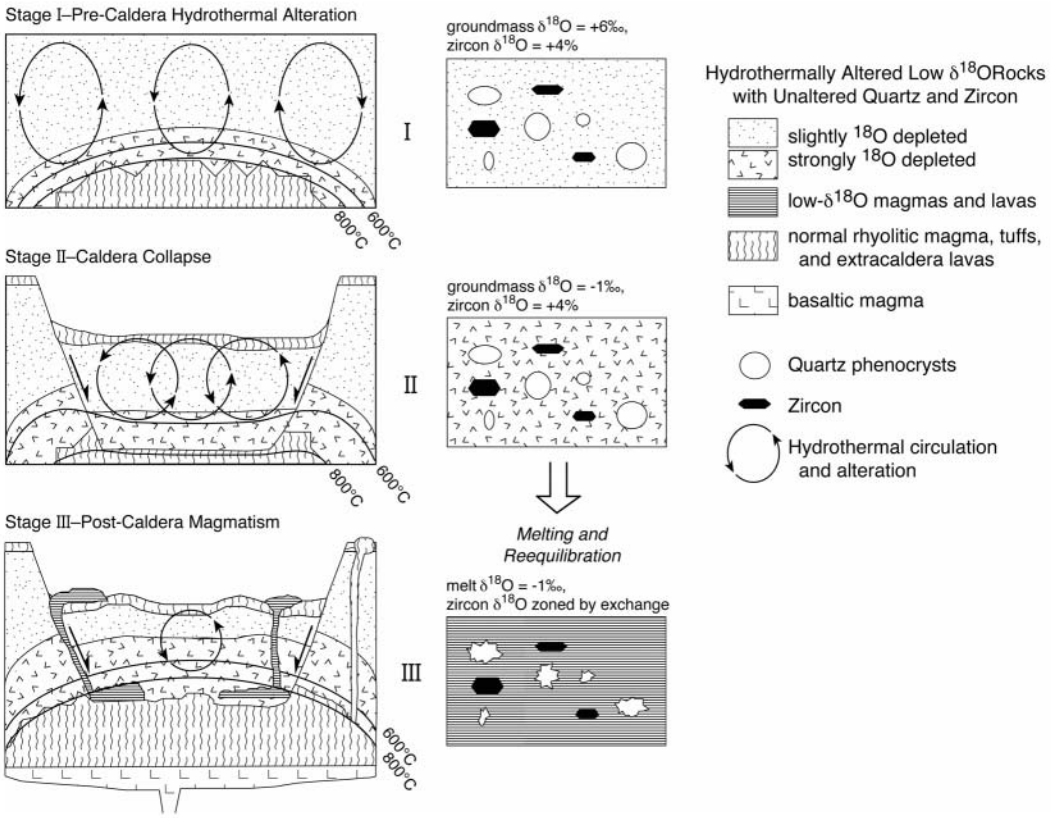

Figure 25. The bulk melting-caldera collapse model for generation of low $\delta^{18}O$ rhyolite. Stage I: hydrothermal alteration creates low $\delta^{18}O$ halo around earlier magma chamber. Quartz and zircon are not affected and retain normal $\delta^{18}O$. Stage II: Down drop of roof during caldera collapse brings altered, low $\delta^{18}O$ lavas from earlier eruptions into contact with high temperature melt remaining in magma chamber. Melting of the altered lavas creates a low $\delta^{18}O$ rhyolitic magma with normal $\delta^{18}O$ xenocrysts of zircon and quartz. Stage III: Some low $\delta^{18}O$ melts are isolated from the magma chamber and erupt as individual, small, post-caldera lavas (from Bindeman and Valley 2001).

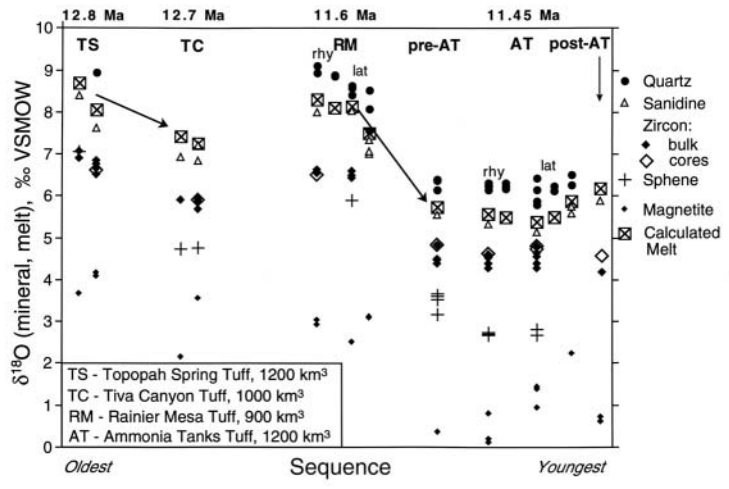

Figure 26. Evolution of $\delta^{18}O$ in minerals and melt for the four major caldera forming tuffs of the Timber Mountain/ Oasis Valley caldera complex. Data within each tuff are separated to show the early rhyolites and late higher temperature latites. Eruptions were paired, a normal $\delta^{18}O$ magma followed 0.1 Myr later by a significantly lower $\delta^{18}O$ magma. The Ammonia Tanks Tuff (AT) at 11.45 Ma is a low $\delta^{18}O$ rhyolite. Air-abraded cores of zircons are higher in $\delta^{18}O$ than bulk zircon concentrates or small zircons from AT, pre-AT or post AT lavas (from Bindeman and Valley 2003).

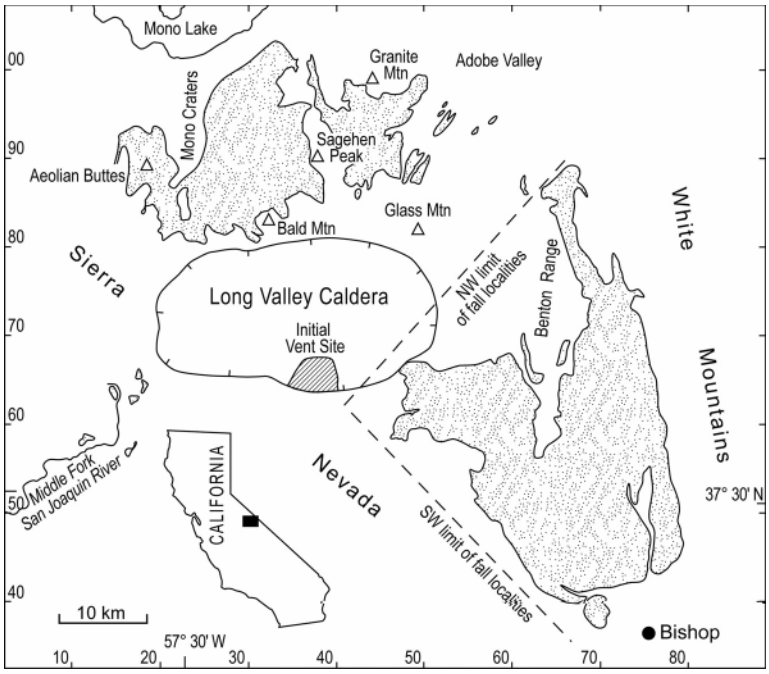

Figure 27. The Long Valley caldera and vicinity, California. Outcrop of the Bishop Tuff ash flow is stippled. The early phases of the Bishop Tuff erupted from the "initial vent site." The total erupted volume was 650 km^3 at 760 ka (from Wilson and Hildreth 1997).

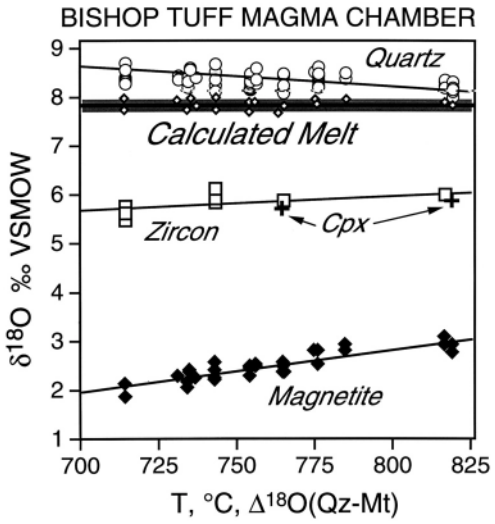

Figure 28. Values of $\delta^{18}O$ for quartz, magnetite, clinopyroxene, and zircon vs. temperature estimated from $\Delta^{18}O$(Qt-Mt) for the Bishop Tuff. The values of $\delta^{18}O$(melt) are remarkably constant (7.80±0.05‰) as calculated from $\delta^{18}O$(Zc) at the Qt-Mt temperature. The range of $\delta^{18}O$(Qt) and (Mt) values reflects exchange with a magma of constant $\delta^{18}O$(WR) and variable temperature (from Bindeman and Valley 2002).

isotope shifts are smaller, but the quantities of low $\delta^{18}O$ melt are larger.

The zoning of $\delta^{18}O$ seen in zircons from the Timber Mountain complex would be consistent with a residence time of approximately 10-15 ky for the normal $\delta^{18}O$ zircon xenocrysts in low $\delta^{18}O$ magmas. This is longer than the residence times inferred from zoning for zircons at Yellowstone, but shorter than the time intervals between successive caldera-forming eruptions i.e., Ammonia Tanks after Rainier Mesa Tuffs. This study demonstrates that large volume, high and low $\delta^{18}O$ magmas can be generated remarkable quickly without oxygen isotopic equilibration of xenocrystic material.

Bishop Tuff, Long Valley caldera

The Bishop Tuff erupted (~650 km^3) in about one week from the Long Valley caldera at 0.76 Ma (Fig. 27). In spite of the climactic nature of the eruption, a clear volcanic stratigraphy exists for units subdividing the tuff (Wilson and Hildreth 1997). Temperature estimates for the magma based on $\Delta^{18}O$(Qt-Mt) (Fig. 28) increase from 715°C for the earliest tuffs (top of the magma chamber) to 815°C for late Bishop Tuff (deepest in the cham-

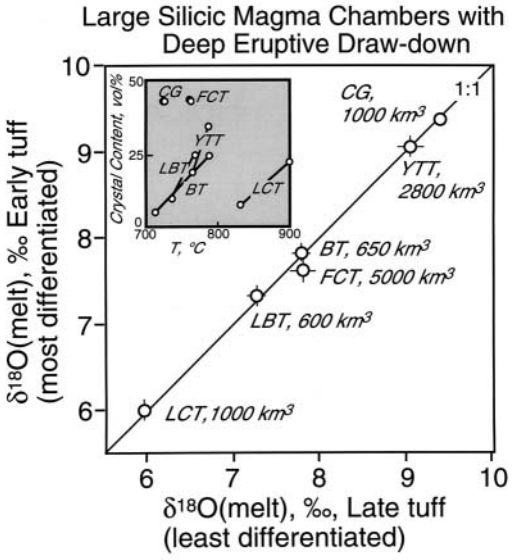

Figure 29. Oxygen isotope values calculated from $\delta^{18}O(Zc)$ for the early, most differentiated and late, least differentiated portions of major Quaternary ash flow tuffs. The good 1:1 correlation demonstrates vertical homogeneity of $\delta^{18}O$ within the magma chambers. BT = Bishop Tuff; CG = Cerro Galan; FCT = Fish Canyon Tuff; LBT = Lower Bandelier Tuff; LCT = Lava Creek Tuff; YTT = youngest Toba Tuff (from Bindeman and Valley 2003).

ber, Bindeman and Valley 2002). The oxygen isotope fractionations decrease smoothly for quartz, zircon and magnetite in response to this temperature increase, however the $\delta^{18}O$ of the magma remained constant, indicating that the Bishop Tuff magma chamber was homogeneous in $\delta^{18}O$ (Fig. 28). Such vertical homogeneity is estimated for at least five other Tertiary caldera-forming tuffs suggesting long-lived magmas and convective stirring processes that homogenized magma chambers (Fig. 29). It is further suggested that granitic batholiths worldwide could initially be homogeneous in $\delta^{18}O$ due to convection.

PHANEROZOIC GRANITES

British Tertiary Igneous Province

The felsic to mafic plutons and lavas of the British Tertiary Igneous Province relate to the opening of the N. Atlantic, outcrop along the coasts of Scotland and Ireland, and stitch across Archean, Proterozoic, and Paleozoic basement (Fig. 30). A classic bulls-eye pattern of low $\delta^{18}O$ surrounds many of the intrusive complexes due to post-magmatic hydrothermal alteration involving large fluxes of heated meteoric water in a shallow sub-volcanic environment (Fig. 31, Forester and Taylor 1977). However, the possibility of low $\delta^{18}O$ magmas and the genesis of the bimodal magmatism have been uncertain.

Magmatic zircons were separated and analyzed along with quartz from granites on Arran, Mull, and the four intrusive centers on Skye (Fig. 32; Gilliam and Valley 1997, Monani and Valley 2001). A majority of the zircon and quartz has $\delta^{18}O$ lower than the mantle value. The low $\delta^{18}O(Zc)$ values were evaluated for exchange with low $\delta^{18}O$ meteoric water by several tests. Imaging by CL and BSE shows typical magmatic growth patterns within euhedral grains. Analysis of zircons of different size or magnetism show no variability as predicted for subsolidus exchange. The fractionation $\Delta(Qt\text{-}Zc)$ does not correlate to $\delta^{18}O(Zc)$ as would be predicted for hydrothermal exchange and disequilibrium. Zircons separated from widely spaced localities within individual granite bodies of the Eastern Red Hills are identical in $\delta^{18}O$ even though the different bodies vary in $\delta^{18}O(Zc)$ from >5 to <0‰ (Fig. 32; #15, 16). Individual zircons analyzed by ion microprobe from single hand samples show no variability in $\delta^{18}O$. Thus, much of the $^{18}O/^{16}O$ depletion of granites from the Isle of Skye is magmatic in origin due to input from the crust. The subsequent low $\delta^{18}O$ hydrothermal overprint on feldspars and quartz is much less intense than has been thought previously.

The amount of crustal input required to generate the low $\delta^{18}O(Zc)$ values of 0 to 1‰ ($\delta^{18}O(WR)$ ~ 2‰, Glas Beinn Mohr granite, #15; Fig. 32) is greater than 40%, exceeding the energy budget of assimilation and suggesting that wholesale melting of granitic material was caused by mafic intrusions at depth. The $\delta^{18}O$ estimate differs from estimates based on trace elements and radiogenic isotopes. These other estimates support the hypothesis that granites were formed by differentiation of mantle melts with ≤10% crustal input and that there was an increasing percentage from the upper

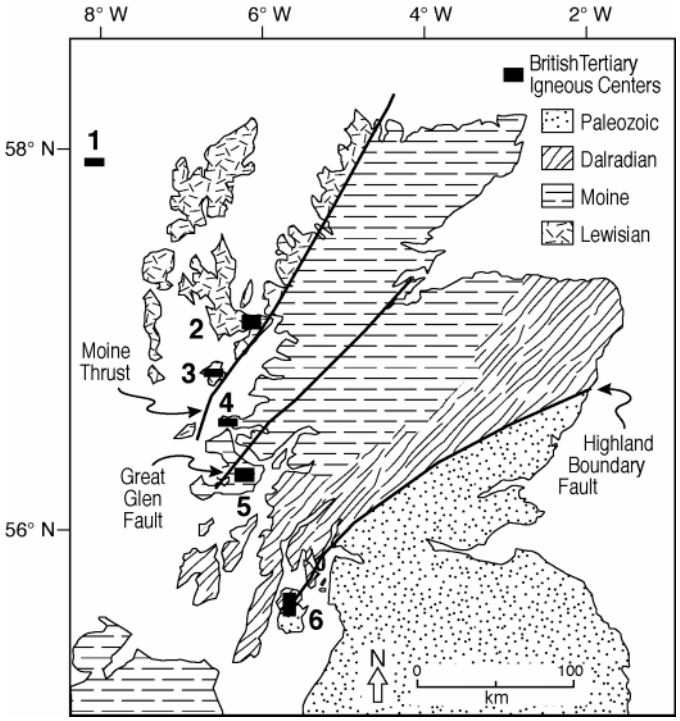

Figure 30. The British Tertiary Igneous Province intrudes Archean to Paleozoic terranes of western Scotland: 1. St. Kilda, 2. Skye, 3. Rhum, 4. Ardnamurchan, 5. Mull, 6. Arran (from Monani and Valley 2001).

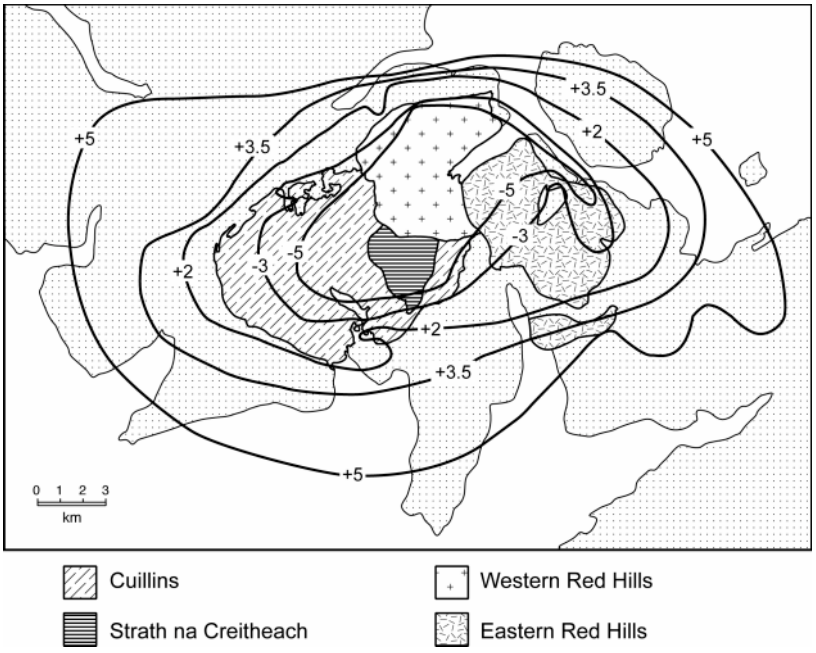

Figure 31. Contours of $\delta^{18}O$ from whole rock samples of basalt and mafic dikes, Isle of Skye. The bulls-eye pattern reflects the intensity of hydrothermal exchange with heated meteoric waters. Circulation of hydrothermal fluids was driven by heat from the four magmatic centers on Skye: the Cuillins, Strath na Creitheach, and the Western and Eastern Red Hills (from Forester and Taylor 1977).

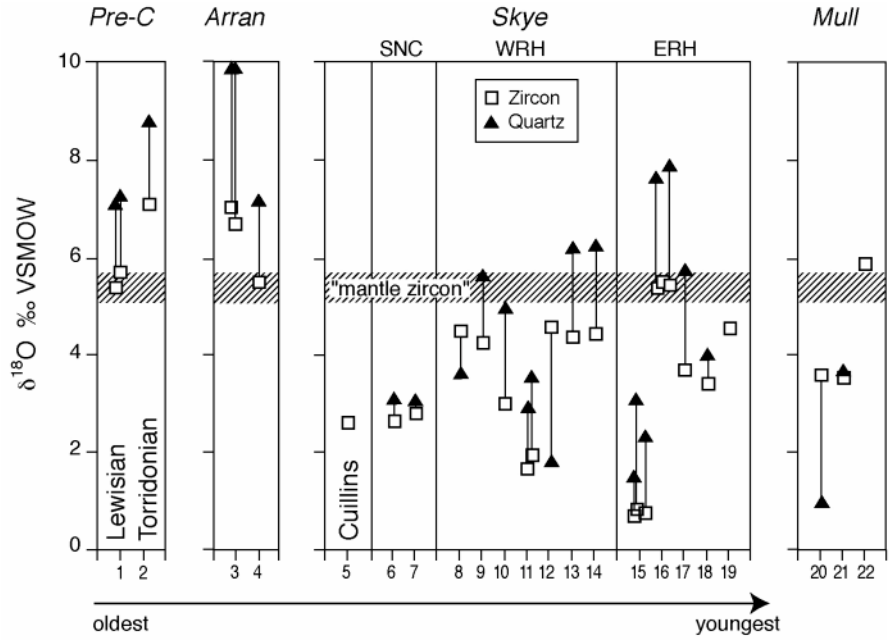

Figure 32. Values of $\delta^{18}O$ for zircon and quartz from granitic rocks of the British Tertiary Igneous Province. Granitic centers on the Isle of Skye are: SNC Strath na Creitheach, WRH Western Red Hills and ERH Eastern Red Hills. Values of $\delta^{18}O(Zc)$ are low indicating intrusion as low $\delta^{18}O$ magmas. Values of $\delta^{18}O(Qt)$ are not generally in equilibrium with zircon due to high temperature hydrothermal alteration of quartz (from Monani and Valley 2001).

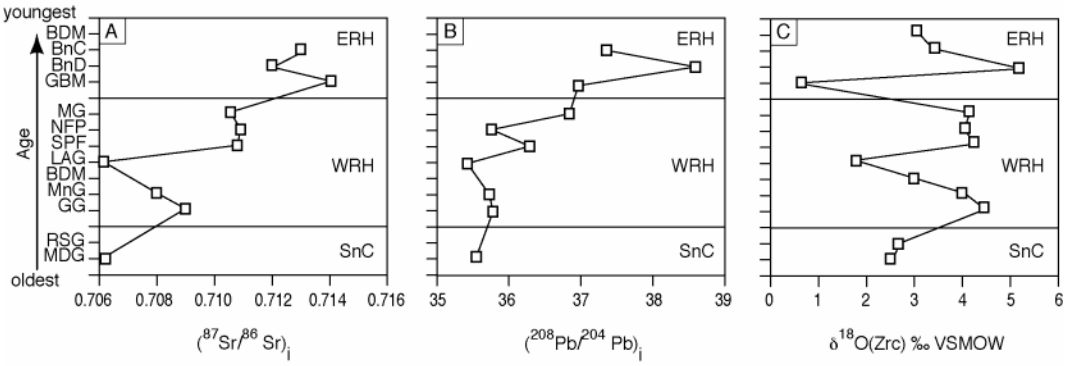

Figure 33. Initial Pb and Sr isotope ratios for whole rock samples of Skye granites (Dickin 1981, Dickin et al. 1984) and $\delta^{18}O(Zc)$ (Monani and Valley 2001) vs. relative age of intrusion. The three granitic centers on Skye are SNC, WRH, and ERH (defined in Fig. 32) (from Monani and Valley 2001).

crust (Fig. 33A,B; Dickin 1981, Dickin et al. 1984). This trend is not evident in the magmatic $\delta^{18}O$ values (Fig. 33C; Monani and Valley 2001) suggesting that $\delta^{18}O$ is decoupled from Sr and Pb because remelting of hydrothermally altered granites within a single suite can significantly impact $\delta^{18}O$ without affecting other geochemical systems.

The low $\delta^{18}O$ Red Hills granites on Skye provide an eroded view of the plutonic roots of a caldera environment like Yellowstone. Repeated magmatism within a shallow stationary center creates the perfect environment for hydrothermal alteration of early units, which are then available for remelting. The resultant recycled component may be indistinguishable with most geochemical

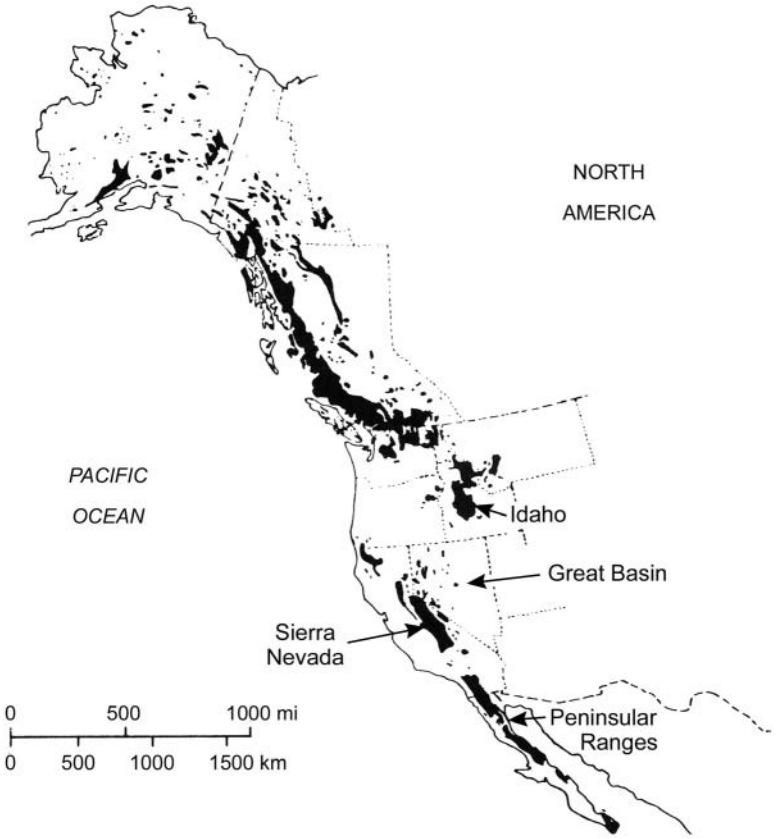

Figure 34. Major Cenozoic and Mesozoic batholiths of North America (black) (from Taylor 1986).

systems and is best resolved with stable isotopes ($\delta^{18}O$ and δD). Such magmatic "cannibalization" may be far more common than is generally recognized with important implications for the thermal budget of the crust.

Mesozoic and Cenozoic granites of the western United States

Idaho batholith. The late Cretaceous and Tertiary granitic rocks of the Idaho batholith (Fig. 34) are intruded into the Precambrian margin of North America. Most rocks intrude Precambrian basement, but west of the Salmon River suture zone, granites intrude Triassic/Jurassic accreted terranes. The edge of the craton is marked by a sharp eastward increase in $^{87}Sr/^{86}Sr_i$ from 0.704 to 0.708 (the "0.706 line," Fig. 35), a decrease in ε_{Nd} from ca. +6 to –16, and an increase in $\delta^{18}O$(WR) from 7 to 10‰ (Fig. 36) (Fleck and Criss 1985, Fleck 1990, King et al. 2003a).

The igneous values of $\delta^{18}O$ and δD are overprinted in some minerals from most samples of the Idaho batholith by post magmatic exchange with heated meteoric water, especially near shallow Eocene plutons (Criss and Taylor 1983, Criss and Fleck 1990, Larson and Geist 1995, King and Valley 2001). Analysis of $\delta^{18}O$ in zircons records preserved magmatic values. The contrast with other minerals shows that details of the magmatic history have been obscured by the later alteration (King and Valley 2001). Values of $\delta^{18}O$(Zc) are relatively constant throughout the batholith in spite of a prolonged history of multiple intrusive pulses, and variable mineralogy, chemistry, and age. The northern lobe (Bitterroot) has an average $\delta^{18}O$(Zc) = 7.1±0.3‰, the southern lobe (Atlanta) is 7.0±1.0‰, and Eocene plutons are 7.2±0.2‰ with the exception of the Casto pluton, which is a low

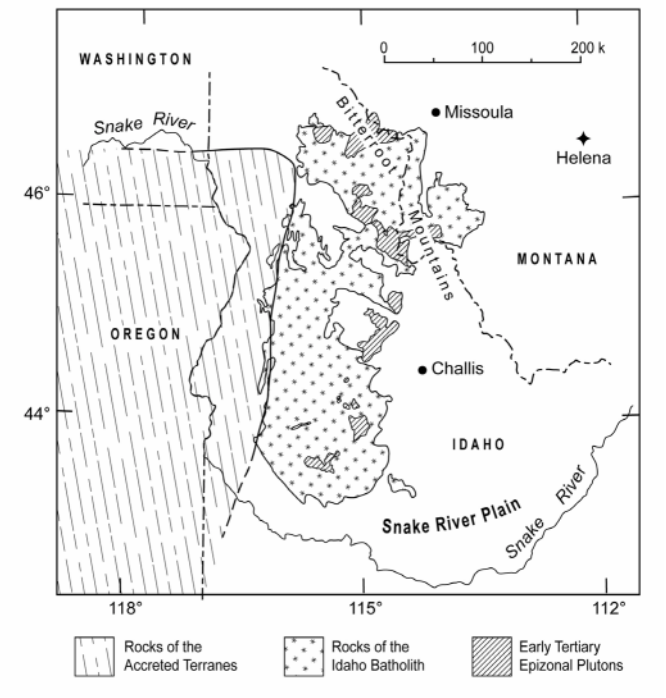

Figure 35. The Idaho batholith (stipple) and surrounding area. The solid curve along the west side of the batholith is the $Sr_i = 0.706$ line. Precambrian continental crust forms basement to the east. Accreted terranes to the west are late Paleozoic and early Mesozoic (from Fleck and Criss 1985).

$\delta^{18}O$ granite ($\delta^{18}O(Zc) = 4.0‰$; $\delta^{18}O(WR) \sim 5.5‰$). Thus, the initial magmatic $\delta^{18}O(WR)$ for most of the batholith was normal at ~8.5‰ and less variable than previously thought. However, small amounts of metasedimentary assimilation are "caught in the act" of elevating $\delta^{18}O$ by analysis of igneous garnets crystallized later and coexisting with zircons (Fig. 8). Presumably, this approach for studying contamination will also reveal differences in trace elements and other geochemical systems.

Great Basin. The Great Basin of Nevada and Utah (Fig. 34) has undergone pulses of compressional and extensional tectonics, and extensive granitic plutonism. Numerous studies of this area have employed radiogenic and stable isotopes to document major crustal boundaries including the edge of the Precambrian craton (Fig. 37). Figure 37A shows Pb isotope zones (Zartman 1974), and isopleths for $^{87}Sr/^{86}Sr_i = 0.706$, $^{87}Sr/^{86}Sr_i = 0.708$ (Kistler and Peterman 1973), and $\varepsilon_{Nd} = -7$ (Farmer and DePaolo 1983). Figure 37B shows the three sub-divisions of Solomon and Taylor (1989) based on analysis of $\delta^{18}O$ in whole rock powders. The radiogenic data mark the cratonic margin at the 0.708 line with continental sediments grading into volcanic arc and ocean floor lithologies farther west. However, no oxygen isotope discontinuities have been found that coincide with the major radiogenic isotope boundaries.

King et al. (2003b) analyzed $\delta^{18}O$ in zircon, titanite, and/or quartz in 275 plutonic rocks from the Great Basin. The faithfulness with which each mineral has preserved magmatic $\delta^{18}O$ decreases: zircon > titanite > quartz. The data from these minerals gives sharper and more accurate trends in magmatic $\delta^{18}O$ than whole rock compositions, which are easily overprinted by alteration of feldspar. Granites of all ages show a difference in $\delta^{18}O(Zc)$ across the 0.706 line, but this is most pronounced in Cretaceous granites for which there is little overlap in data (Fig. 38). Thus oxygen isotope discontinuities do correlate with radiogenic isotope boundaries if the effects of postmagmatic exchange are properly recognized.

Sierra Nevada. The oxygen isotope geochemistry of magmas of the Sierra Nevada batholith has long been a puzzle. Dramatic trends are seen in the Peninsular Ranges batholith farther south (Fig. 34) with $\delta^{18}O(WR)$ increasing west to east (Taylor 1986), and correlations of $\delta^{18}O$ to tectonic setting are described in the Idaho batholith and among plutons of the Great Basin. However, the variability of $\delta^{18}O$ within the Sierra Nevada has seemed erratic and uncorrelated with geologic features (Masi et al. 1981, Ross 1983). Complex relations in the Sierras could result from a number of factors including: post magmatic alteration, different contributions of continental vs. oceanic basement, the presence of granites from an earlier Jurassic arc, and variable amounts of uplift of a

vertically variable $\delta^{18}O$ profile in the Sierran Arc.

Lackey et al. (2001) report $\delta^{18}O$ of zircons from samples that were previously analyzed for U-Pb age, initial Pb isotope ratios, and $^{87}Sr/^{86}Sr_i$ (Chen and Moore 1982, Chen and Tilton 1991). At the latitude of Sequoia National Park (36.5° N), $\delta^{18}O(Zc)$ increases from 5.8 to 8.0, west to east in the western 40 km of the batholith and correlates with Sr and Pb isotopes. The positive correlation of $^{87}Sr/^{86}Sr_i$ and $\delta^{18}O$ is similar to the Peninsular Ranges batholith. The 0.706 line runs approximately N-S and crosses this 40-km traverse midway. West of 0.706, granites are in the Weakly Contaminated zone and to the east they are in the Strongly Contaminated-Reduced zone of Ague and Brimhall (1988). These zones are distinct in $^{206}Pb/^{204}Pb$ as well as $\delta^{18}O$: 18.658-18.741 and 5.9-7.0‰ in the west vs. 18.929-19.254 and 6.8-7.4‰ in the east. These differences are consistent with contamination by high $\delta^{18}O$ Kings sequence metasediments to the east. Contamination of some magmas by high $\delta^{18}O$ material west of the 0.706 line is observed in the zircon data, but was previously unrecognized by radiogenic isotope studies.

The depths of crystallization for Sierran granites are inferred from Al-in-hornblende barometry to increase from generally 3-6 km in the central and northern parts of the batholith to 30 km in the Tehachapi Mountains in the south. Lackey et al. (2003) show that $\delta^{18}O(Zc)$ in the Tehachapi/Lake Isabella regions is significantly higher than in the rest of the batholith, 7.8±0.8‰ vs. 6.1±0.8‰ (Fig. 39) suggesting that magmas of the southern Sierras were contaminated by significant amounts of high $\delta^{18}O$ material not seen in exposed portions of the batholith elsewhere. Comparison of $^{87}Sr/^{86}Sr_i$ and ε_{Nd} to $\delta^{18}O$ suggests that the high $\delta^{18}O$ material was hydrothermally altered ocean crust or volcanic arc sediments.

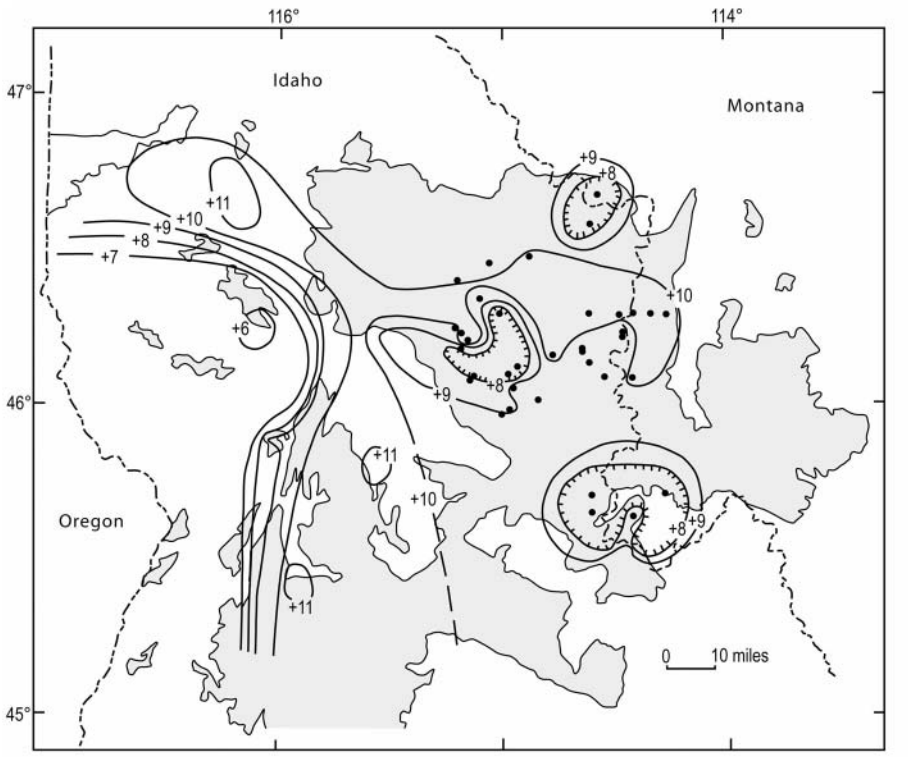

Figure 36. Contours of plutonic $\delta^{18}O(WR)$ in the Idaho Batholith and vicinity. Isopleths of $\delta^{18}O$ = 8-9‰ coincide with the Sr_i = 0.706 line (Fig. 35). The hachured regions within the batholith mark areas of post-magmatic alteration of whole rock compositions by interaction with heated meteoric water (from Fleck and Criss 1985).

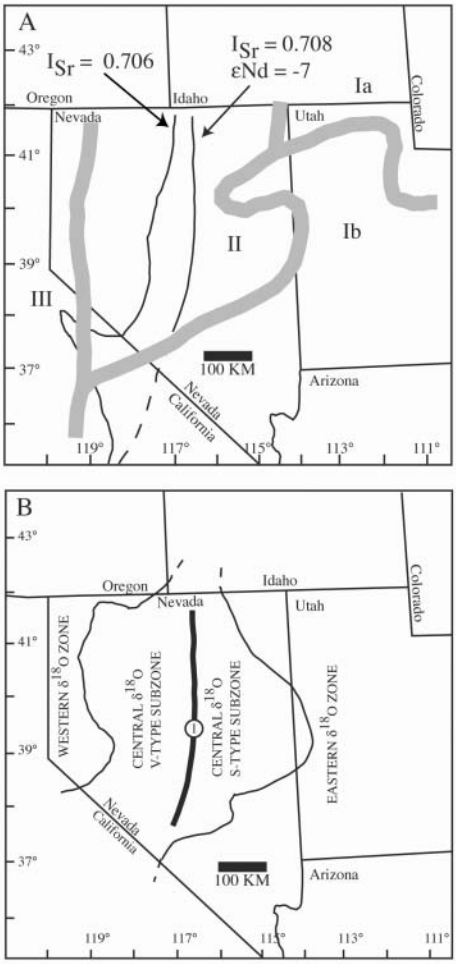

Figure 37. Isotopic discontinuities in plutonic rocks of the western United States. (A) Sr_i = 0.706 and 0.708, and ε_{Nd} = –7 lines, and Pb isotope zones Ia, Ib, II, and III. The region between the 0.706 and 0.708 lines is the transition between Precambrian continental crust to the east, and arc rocks to the west. (B) the western, central and eastern $\delta^{18}O$ zones of Solomon and Taylor (1989) based on analysis of whole rock powders. The heavy line marked 1 is ε_{Nd} = –7. (from King et al. 2003b).

A-type granites, northeastern China

Phanerozoic granites represent 50-80% of mountainous areas in the Central Asian Orogenic Belt of northeastern China (Fig. 40). These rocks represent major pulses of I- and A-type plutonism in the Late Paleozoic to Late Mesozoic that are proposed to represent juvenile additions to crustal growth (Wu et al. 2000, 2002). Many granites have relatively low $^{87}Sr/^{86}Sr_i$ of 0.705, positive ε_{Nd} of 0 to +4, model T_{DM} ages of 1.3 to 0.5 Ga suggesting a dominantly primitive source; some granites that intrude Precambrian country rocks have negative ε_{Nd} and older T_{DM} suggesting involvement of Precambrian basement. These plutons are proposed to have formed in a post- or anorogenic tectonic setting. The primitive source rocks have been proposed to be either: (1) underplated basaltic melts near the base of the crust or (2) subducted ocean crust within the mantle (Wu et al. 2000, 2002; Wei et al. 2002). This distinction is important for models of crustal growth.

The Nianzishan granite is located in northeastern China (Fig. 40) and is representative of late Cretaceous A-type granites that most likely related to extension and rifting along the continental margin of eastern China in the southeastern part of the Central Asian Orogenic Belt (Wang et al. 1995, Wu et al. 2002, Wei et al. 2002, 2003). Minerals include quartz, K-feldspar, Na-amphibole, pyroxene, magnetite and zircon. Positive values of ε_{Nd} (+4.27 to +0.86) and relatively young Nd model ages of 846-569 Ma suggest a significant mantle component to magmas. Miarolitic cavities and low $\delta^{18}O$(WR) (4.3 to –1.5‰) suggest intrusion at shallow levels in the crust and hydrothermal alteration by heated meteoric waters (see, Sheppard 1986). More recently, analysis of $\delta^{18}O$(Zc) reveals values of 4.2 to 3.1, showing that magmas were low in $\delta^{18}O$ before crystallization and documenting previously unrecognized remelting of hydrothermally altered oceanic or continental crust (Wei et al. 2002, 2003).

Cenozoic granitoids of the Antarctic Peninsula

Bolz (2001) reports ion microprobe analyses of zircons from two granites and a diorite (120-80 Ma) of the Rymill Coast and Eternity Range on the Antarctic Peninsula. Values of $\delta^{18}O$ for plagioclase, hornblende and biotite range from –4.6 to 0.7‰ due to high temperature exchange with meteoric water. Analyses of quartz range from 3.9 to 5.3‰ also due to alteration. In contrast to these variable and low values, the values of $\delta^{18}O$(Zc) for the three plutons are constant and mantle-like at 5.1-5.5‰. Individual spot analyses show no variability from zircon to zircon within the ±1‰ (1sd) precision of the SIMS data.

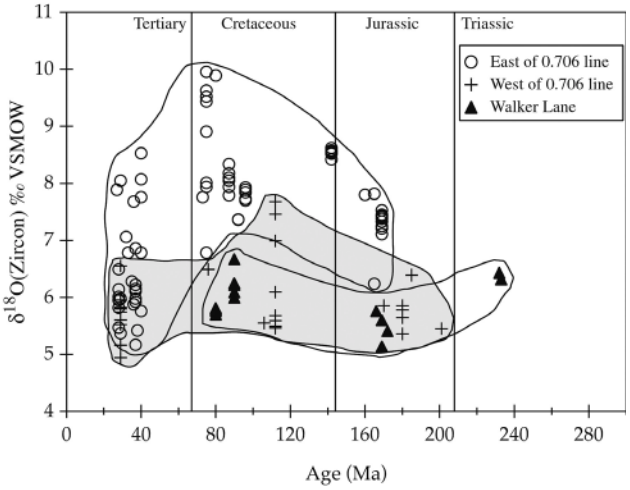

Figure 38. Values of $\delta^{18}O$(Zc) vs. age of pluton for granitic rocks of the Great Basin, western United States. Values east of the 0.706 line (open circles) are higher than to the west (crosses and triangles). East of the 0.706 line, $\delta^{18}O$ increases from Jurassic through Cretaceous. After 70 Ma and a break in plutonism, $\delta^{18}O$ returns to lower values. These trends are not seen in whole rock data (from King et al. 2003b).

Fe-oxide melt in syenitic xenoliths

Globules of Fe-Ti-oxide melt in mafic to felsic xenoliths within Tertiary alkali basalts of the Carpathians are proposed to form by liquid immiscibility (Hurai et al. 1998). High iron oxide melt globules are found encased in glass pockets and within rock forming plagioclase and zircon. The $\delta^{18}O$(Zc) values of 5.1-5.6‰ are the same as mafic minerals and calcic plagioclase (4.9-5.9‰) from gabbroic xenoliths supporting a common mantle source for the Fe-oxide melt containing xenoliths.

Magmatic epidote-bearing granitoids

Epidote in granitic rocks has been studied in detail to distinguish magmatic epidote, which has importance for estimation of pressure, water activity and uplift rates, from hydrothermal epidote, which records later, post-magmatic history.

Keane and Morrison (1997) studied four textural varieties of epidote in quartz monzonite of the Triassic Mt. Lowe intrusion, San Gabriel Mts., California. Three of these varieties show textural evidence of being magmatic: coarse euhedral and anhedral grains, and intergrowths showing crystal faces against hornblende or biotite. Only epidote in cross-cutting veins is clearly post-magmatic. However, microanalysis of $\delta^{18}O$(epidote) shows that both euhedral and anhedral epidote can be partially altered or exchanged. The

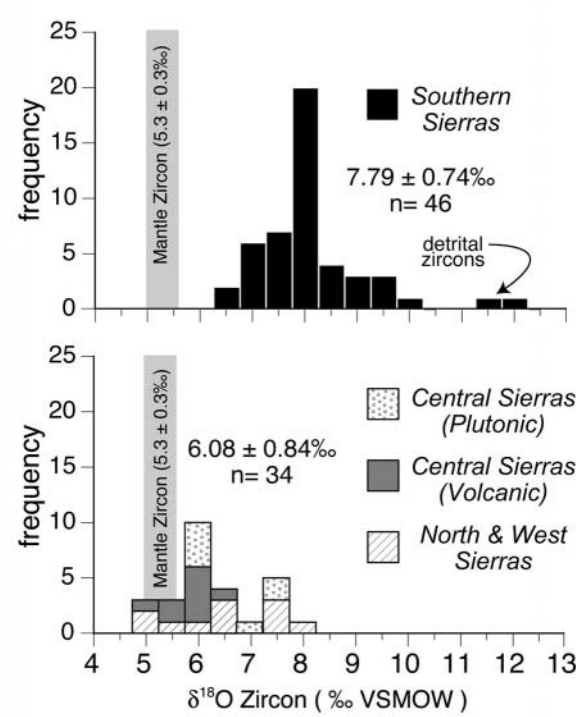

Figure 39. Oxygen isotope compositions of zircon from the Sierra Nevada batholith. Samples from the deeply exhumed (up to 30 km) southern portion of the batholith average over 1.5‰ higher $\delta^{18}O$ than the shallower 3-7 km rocks farther north. Granulite facies country rocks in the south are migmatitic suggesting that the deep portions of the batholith were contaminated by high $\delta^{18}O$ crust (from Lackey et al. 2003).

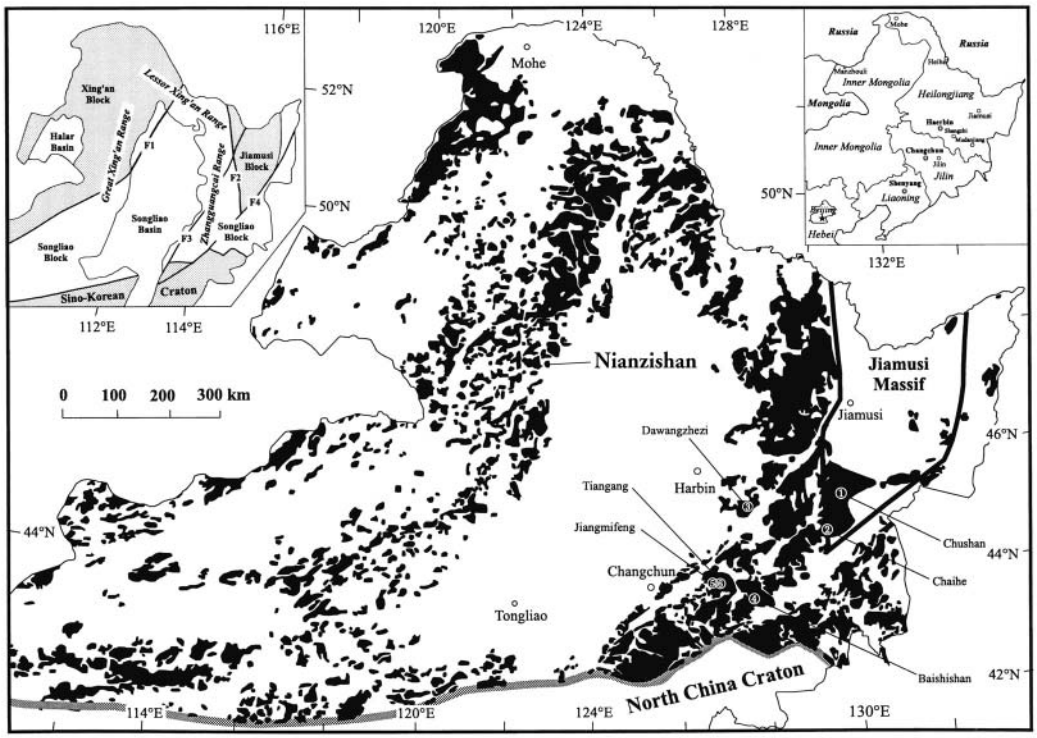

Figure 40. Phanerozoic granites of northeastern China occupy 50-80% of the exposed areas of mountains. F1, F2, F3, and F4 (inset) are the Nenjiang, Mudanjiang, Jiayi, and Dunmi Faults, respectively (from Wu et al. 2000).

euhedral grains are bimodal, $\delta^{18}O$ = 5.36±0.13‰ and 4.66±0.23‰. Analysis of magmatic zircons yields 5.70±0.15‰ suggesting that the values above 5‰ are magmatic and that lower values reflect subsolidus exchange. Thus, use of textural criteria alone can be misleading.

The Neoproterozoic Borborema province, northeastern Brazil contains a large volume of diverse granitic rocks recording two orogenic cycles: Cariris Velhos (1.1-0.95 Ga) and Brasiliano (0.73-0.52 Ga) (Fig. 41). Magmatic epidote is found in calc-alkalic, shoshonitic, and trondhjemitic granitoids in five tectonostratigraphic terranes of the province (Ferreira et al. 1998, Sial et al. 1999).

Ferreira et al. (2003) compared magmatic epidote, titanite, and zircon from two contrasting metaluminous granitoids that crystallized at different depths, Emas and Sao Rafael. Values of $\Delta^{18}O$(zircon-titanite) yield magmatic temperatures, but $\Delta^{18}O$ (quartz-magmatic epidote) and $\Delta^{18}O$(zircon-epidote) are self-consistent, and larger than predicted for magmatic temperatures. These fractionations suggest continuous, closed-system, sub-solidus exchange among all minerals except zircon and titanite. Values of $\delta^{18}O$(WR) were determined by analysis of $\delta^{18}O$(Zc) and calculation of $\delta^{18}O$(WR) based on the mineral mode.

Paradoxically, the Emas pluton has many I-type characteristics, but high $\delta^{18}O$(WR) = 11.6‰, while the Sao Rafael has Sr and Nd characteristics of S-type and low $\delta^{18}O$ = 7.9‰. Typically, the higher $\delta^{18}O$ values would be thought of as sediment derived. The reversal of values of $\delta^{18}O$(WR) thus indicates that systematics of oxygen isotopes are not coupled to radiogenic isotopes in these rocks. This can be explained if fluid-hosted processes such as hydrothermal exchange have altered the $\delta^{18}O$ of source rocks. If source rocks are magmatic and young at the time of melting, there may not be a radiogenic isotope contrast and the only signature of crustal recycling will be from stable isotopes. Several of the studies reviewed above support this conclusion and suggest that crustal recycling is more important than has generally been recognized.

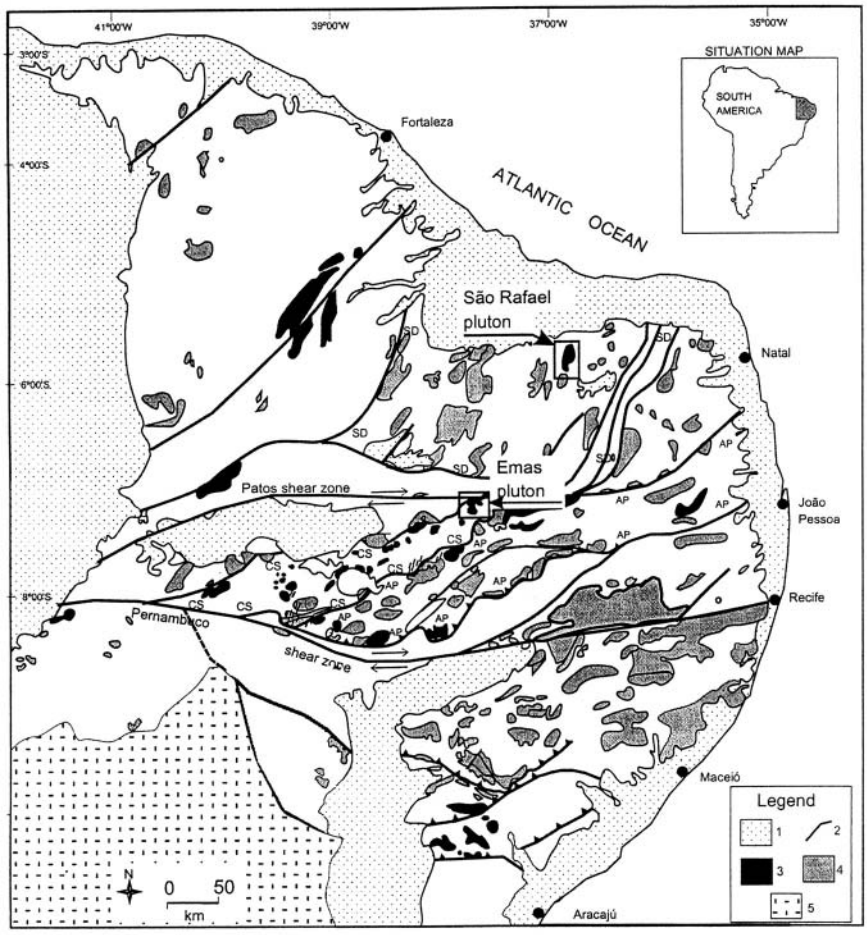

Figure 41. Granitoids of the Neoproterozoic Borborema province, Brazil. The Brasiliano-age Emas and Sao Rafael plutons are shown. 1 = Phanerozoic cover; 2 = major shear zones and terrane boundaries; 3 = magmatic epidote-bearing granitoids; 4 = other granitoids; 5 = Sao Francisco craton; SD = Serido terrane; CS = Cachoeirinha-Salgueiro terrane; AP = Alto Pajeu terrane (from Ferreira et al. 2003).

ACKNOWLEDGMENTS

Pat Bickford, Ilya Bindeman, Aaron Cavosie, Cory Clechenko, Val Ferreira, John Hanchar, Liz King, Jade Star Lackey, William Peck, and Doug Rumble made perceptive comments on this paper. Mary Diman helped with drafting. NSF and DOE are thanked for supporting this research.

REFERENCES

Ague JJ, Brimhall GH (1988) Regional variations in bulk chemistry, mineralogy, and compositions of mafic and accessory minerals in the batholiths of California. Geol Soc Am Bull 100:891-911

Ague JJ, Brimhall GH (1988) Magmatic arc asymmetry and distribution of anomalous plutonic belts in the batholiths of California: Effects of assimilation, crustal thickness, and depth of crystallization. Geol Soc Am Bull 100:912-927

Ashwal LD (1993) Anorthosites. Springer, Berlin, 422 p

Bacon CR, Adami LH, Lanphere MA (1989) Direct evidence for the origin of low-^{18}O silicic magmas: quenched samples of a magma chamber's partially-fused granitoid walls, Crater Lake, Oregon. Earth Planet Sci Lett 96:199-208

Balan E, Neuville DR, Trocellier P, Fritsch E, Muller JP, Calas G (2001) Metamictization and chemical durability of

detrital zircon. Am Mineral 86:1025-1033
Beatty DW, Taylor HP Jr, Coad PR (1988) An oxygen isotope study of the Kidd Creek, Ontario, volcanogenic massive sulfide deposits:evidence for a high ^{18}O ore fluid. Econ Geol 83:1-17
Bibikova YV, Ustinov VI, Gracheva TV, Kiselevskiy MA, Shukolyukov YA (1982) Variations of isotope distribution in oxygen of accessory zircons. Doklady Akad. Nauk SSSR 264:698-700
Bindeman IN (2003) Crystal sizes in evolving silicic magma chambers. Geology 31 (in press)
Bindeman IN, Valley JW (2000a) Formation of low-$\delta^{18}O$ rhyolites after caldera collapse at Yellowstone, Wyoming, USA. Geology 28:719-722
Bindeman IN, Valley JW (2000b) Oxygen isotope study of accessory zircon, sphene and other minerals in carbonate cement of Trench 14, Yucca Mountain: No evidence for hydrothermal origin. Geol Soc Am Abstr Prog A-261
Bindeman IN, Valley JW (2001) Low $\delta^{18}O$ rhyolites from Yellowstone: Magmatic evolution based on analysis of zircons and individual phenocrysts. J Petrol 42:1491-1517
Bindeman IN, Valley JW (2002) Oxygen isotope study of the Long Valley magma system, California: Isotope thermometry and convection in large silicic magma bodies. Contrib Mineral Petrol 144:185-205
Bindeman IN, Valley JW (2003) Rapid generation of both high and low-$\delta^{18}O$, large volume silicic magmas at Timber Mountain/Oasis Valley caldera complex, Nevada. Geol Soc Am Bull 115 (in press)
Bindeman IN, Valley JW, Wooden JL, Persing HM (2001a) Post-caldera volcanism: *In situ* measurement of U-Pb age and oxygen isotope ratio in Pleistocene zircons from Yellowstone caldera. Earth Planet Sci Lett 189:197-206
Bolz V (2001) The oxygen isotope geochemistry of zircon as a petrographic tracer in high temperature contact metamorphic and granitic rocks. MS thesis, University of Edinburgh, 208 p
Cavosie AJ, Valley JW, Fournelle J, Wilde SA (2002) Implications for sources of Jack Hills metasediments: Detrital chromite. Geochim Cosmochim Acta 66:A125
Chacko T, Cole DR, Horita J (2001) Equilibrium oxygen, hydrogen and carbon isotope fractionation factors applicable to geologic systems. *In* Valley JW, Cole DR (eds) Stable Isotope Geochemistry. Rev Mineral Geochem 43:1-81
Chen JH, Moore JG (1982) Uranium-lead isotopic ages from the Sierra Nevada batholith, California. J Geophys Res B 87:4761-4784
Chen JH, Tilton GR (1991) Applications of lead and strontium isotopic relationships to the petrogenesis of granitoid rocks, central Sierra Nevada batholith, California. Geol Soc Am Bull 103:437-447
Chiarenzelli JR, McLelland JM (1993) Granulite facies metamorphism, palaeo-isotherms and disturbance of the U-Pb systematics of zircon in anorogenic plutonic rocks from the Adirondack Highlands. J Metamorph Geol 11:59-70
Christiansen RL (2000) The Quaternary and Pliocene Yellowstone Plateau volcanic field of Wyoming, Idaho, and Montana. U S Geol Surv Prof Paper 729-G, 145 p
Clayton RN, Kieffer SW (1991) Oxygen isotopic thermometer calibrations. *In* Taylor HP, O'Neil JR, Kaplan IR (eds) Stable Isotope Geochemistry. Geochem Soc Spec Pub 3:3-10
Clechenko CC, Valley JW, Hamilton MA, McLelland J, Bickford ME (2002) Direct U-Pb dating of the Marcy Anorthosite, Adirondacks, NY, USA. Goldschmidt Conf, Extended Abstr, Geochim Cosmochim Acta 66, Supplement 1:144
Cole DR, Chakraborty S (2001) Rates and mechanisms of isotopic exchange. *In* Valley JW, Cole DR (eds) Stable Isotope Geochemistry. Rev Mineral Geochem 43:83-223
Criss RE, Fleck RJ (1990) Oxygen isotope map of the giant metamorphic-hydrothermal system around the northern part of the Idaho batholith, U.S.A. Appl Geochem 5:641-655
Criss RE, Taylor HP (1983) An $^{18}O/^{16}O$ and D/H study of Tertiary hydrothermal systems in the southern half of the Idaho batholith. Geol Soc Am Bull 94:640-663
Dickin AP (1981) Isotope geochemistry of Tertiary igneous rocks from the Isle of Skye, N.W. Scotland. J Petrol 22:155-189
Dickin AP, Brown LR, Thompson RN, Halliday AN, Morrison MA (1984) Crustal contamination and the granite problem in the British Tertiary volcanic province. *In* Moorbath S, Thompson N, Oxburgh R (eds) The Relative Contributions of Mantle, Oceanic Crust and Continental Crust to Magma Genesis. Royal Soc London 310:755-780
Eiler JM, Valley JW (1994) Preservation of Pre-metamorphic Oxygen Isotope Ratios in Granitic Orthogneiss from the Adirondack Mts., N.Y. Geochim Cosmochim Acta 58:5525 5535
Eiler JM, Baumgartner LP, Valley JW (1992) Intercrystalline stable isotope diffusion: A fast grain boundary model. Contrib Mineral Petrol 112:543-557
Eiler JM, Valley JW, Baumgartner LP (1993) A new look at stable isotope thermometry. Geochim Cosmochim Acta 57:2571-2583
Eiler JM, Graham CM, Valley JW (1997) SIMS analysis of oxygen isotopes: Matrix effects in complex minerals and glasses. Chem Geol 13:221-244
Eiler JM, Farley KA, Valley JW, Hofmann AW, Stolper EM (1996) Oxygen isotope constraints on the sources of Hawaiian volcanism. Earth Planet Sci Lett 144:453-468
Eiler JM, Farley KA, Valley JW, Hauri E, Craig H, Hart SR, Stolper EM (1997) Oxygen isotope variations in Ocean Island Basalts. Geochim Cosmochim Acta 61:2281-2293

Elliot BA, Peck WH, Ramo O, Vaasjoki M, Valley JW (2001) Reconstruction of terrane boundaries in the Finnish Svecofennian: Oxygen isotopes from zircon. Geol Soc Am Abstr Progr 33:264

Farmer GL, DePaolo DJ (1983) Origin of Mesozoic and Tertiary granite in the western United States and implications for Pre-Mesozoic crustal structure: 1. Nd and Sr isotopic studies in the geocline of the northern Great Basin. J Geophys Res 88:3379-3401

Ferreira VP, Sial AN, Jardim de Sa EF (1998) Geochemical and isotopic signatures of Proterozoic granitoids in terranes of the Borborema structural province, northeastern Brazil. J South Am Earth Sci 11:439-455

Ferreira VP, Valley JW, Sial AN, Spicuzza MJ (2003) Oxygen isotope compositions and magmatic epidote from two contrasting metaluminous granitoids, NE Brazil. Contrib Mineral Petrol (in review)

Fleck RJ (1990) Neodymium, strontium, and trace-element evidence of crustal anatexis and magma mixing in the Idaho Batholith. *In* Anderson JL (ed) The Nature and Origin of Cordilleran Magmatism. Geol Soc Am Memoir 174:359-373

Fleck RJ, Criss RE (1985) Strontium and oxygen isotopic variations in Mesozoic and Tertiary plutons of central Idaho. Contrib Mineral Petrol 90:291-308

Fontan F, Monchous P, Autefage F (1980) Presence de zircons hafniferes dans des pegmatites granitiques des Pyrenees Ariegoises. Bull Soc franc Minéral Cristallogr 103:88-91

Forester RW, Taylor HP Jr (1977) $^{18}O/^{16}O$, D/ H, and $^{13}C/^{12}C$ studies of the Tertiary igneous complex of Skye, Scotland. Am J Sci 277:136-177

Fortier SM, Giletti BJ (1989) An empirical model for predicting diffusion coefficients in silicate minerals. Science 245:1481-1484

Fournelle JH, Bindeman I, Donovan JJ, Valley JW (2000) Quantitative EPMA Mapping of Minor and Trace Elements in Zircons from Yellowstone Tuffs and Lavas. EOS Trans Am Geoph Union S26-27

Geisler T, Pidgeon RT (2001) Significance of radiation damage on the integral SEM cathodoluminescence intensity of zircon: An experimental annealing study. N Jb Mineral Mh 10:433-445

Geisler T, Pidgeon RT, van Bronswijk W, Pleysier R (2001) Kinetics of thermal recovery and recrystallization of partially metamict zircon, a Raman spectroscopic study. Eur J Mineral 13:1163-1176

Gilbert B, Frazer BF, Naab F, Fournelle J, Valley JW, De Stasio G (2003) X-ray absorption spectroscopy of silicates for in situ, sub-micrometer mineral identification. Am Mineral (in press)

Gilliam CE, Valley J W (1997) Low $\delta^{18}O$ magma, Isle of Skye, Scotland: Evidence from zircons. Geochim Cosmochim Acta 61:4975-4981

Graham CM, Valley JW, Winter B L (1996) Ion microprobe analysis of $^{18}O/^{16}O$ in authigenic and detrital quartz in St. Peter sandstone, Michigan Basin and Wisconsin Arch, USA: Contrasting diagenetic histories. Geochim Cosmochim Acta 24:5101-5116

Hanchar JM, Miller CF (1993) Zircon zonation patterns as revealed by cathodoluminescence and backscattered electron images: Implications for interpretation of complex crustal histories. Chem Geol 110:1-13

Hanchar JM, Rudnick RL (1995) Revealing hidden structures: The application of cathodoluminescence and backscattered electron imaging to dating zircons from lower crustal xenoliths. Lithos 36:289-303

Hildreth W, Christiansen RL, O'Neil JR (1984) Catastrophic isotopic modification of rhyolitic magma at times of caldera subsidence, Yellowstone Plateau volcanic field. *In* Calderas and Associate Igneous Rocks. Am Geophys Union 89:8339-8369

Hoffbauer R, Hoernes S, Fiorentini E (1994) Oxygen isotope thermometry based on a refined increment method and its applications to granulite-grade rocks from Sri Lanka. Precambrian Res 66:199-220

Hoffman PF, Kaufman AJ, Halverson GP, Schrag DP (1998) A Neoproterozoic snowball Earth. Science 281:1342-1346

Hurai V, Simon K, Wiechert U, Hoefs J, Konecny P, Huraiova M, Pironon J, Lipka J (1998) Immiscible separation of metalliferous Fe/ Ti-oxide melts from fractionating alkali basalt: P-T-f_{O2} conditions and two-liquid elemental partitioning. Contrib Mineral Petrol 133:12-29

Huston DL, Taylor BE, Bleeker W, Watanabe DH (1996) Productivity of volcanic-hosted massive sulfide districts: new constraints from the $\delta^{18}O$ of quartz phenocrysts in cogenetic felsic rocks. Geology 24:459-462

Kamo SL, Davis DW (1994) Reassessment of Archean crustal development in the Barberton Mountainland, South Africa, based on U-Pb dating. Tectonics 13:167-192

Keane SD, Morrison J (1997) Distinguishing magmatic from subsolidus epidote: laser probe oxygen isotope compositions. Contrib Mineral Petrol 126:265-274

Kennedy AK (2000) The search for new zircon standards for SIMS. *In* Woodhead JD, Hergt JM, Nobel WP (eds) Beyond 2000: New Frontiers in Isotope Geoscience. Lorne, 2000, Abstr Proc, p 109-111

Kieffer SW (1982) Thermodynamics and lattice vibrations of minerals: 5, Applications to phase equilibria, isotopic fractionation, and high-pressure thermodynamic properties. Rev Geophys Space Phys 20:827-849

King EM (1997) Oxygen isotope study of igneous rocks from the Superior Province, Canada. MS thesis, University of Wisconsin, Madison, 84 p

King EM (2001) Oxygen isotope study of magmatic source and alteration of granitic rocks in the Western United States and the Superior Province, Canada. PhD dissertation, University of Wisconsin, Madison, 224 p

King EM, Valley JW (2001) Source, magmatic contamination, and alteration of the Idaho batholith. Contrib Mineral

Petrol 142:72-88
King EM, Barrie CT, Valley JW (1997) Hydrothermal alteration of oxygen isotope ratios in quartz phenocrysts, Kidd Creek mine, Ontario: Magmatic values are preserved in zircon. Geology 25:1079-1082
King EM, Barrie CT, Valley JW (1998a) Hydrothermal alteration of oxygen isotope ratios in quartz phenocrysts, Kidd Creek Mine, Ontario: Magmatic values preserved in zircons: Reply. Geology 26:764
King EM, Valley JW, Davis DW, Edwards GR (1998b) Oxygen isotope ratios of Archean plutonic zircons from granite-greenstone belts of the Superior Province: Indicator of magmatic source. Precambrian Res 92:47-67
King EM, Valley JW, Davis DW (2000) Oxygen isotope evolution of volcanic rocks at the Sturgeon Lake volcanic complex, Ontario. Can J Earth Sci 37:39-50
King EM, Valley JW, Davis DW, Kowalis BJ (2001) Empirical determination of oxygen isotope fractionation factors for titanite with respect to zircon and quartz. Geochim Cosmochim Acta 65:3165-3175
King EM, Beard BL, Johnson CM, Valley JW (2003a) Oxygen and strontium isotopic evidence for assimilation and fractional crystallization in the Idaho batholith. Geol Soc Am Bull (in review)
King EM, Valley JW, Stockli DF, Wright JE (2003b) Oxygen isotope trends of granitic magmatism in the Great Basin. (in review)
Kinny PD, Compston W, Bristow JW, Williams IS (1989) Archaean mantle xenocrysts in a Permian kimberlite: Two generations of kimberlitic zircon in Jwaneng DK2, southern Botswana. Geol Soc Australia 14:833-842
Kistler RW, Peterman ZE (1973) Variations in Sr, Rb, K, Na, and initial $^{87}Sr/^{86}Sr$ in Mesozoic granitic rocks and intruded wall rocks in central California. Geol Soc Am Bull 84:3489-3512
Kohn MJ (1999) Why most "dry" rocks should cool "wet." Am Mineral 84:570-580
Kohn MJ, Valley JW (1998) Effects of cation substitutions in garnet and pyroxene on equilibrium oxygen isotope fractionations. J Metamorph Geol 16:625-639
Kresten P, Fels P, Berggren G (1975) Kimberlitic zircons: A possible aid on prospecting for kimberlites. Mineralium Deposita 10:47-56
Krogh TE, Davis GL (1975) Alteration in zircons and differential dissolution of altered and metamict zircon. Ann Rept Geophys Lab Carneg Inst Wash 74:619-622
Krogh TE (1982a) Improved accuracy of U-Pb zircon ages by the creation of more concordant systems using an air abrasion technique. Geochim Cosmochim Acta 46:637-649
Krogh TE (1982b) Improved accuracy of U-Pb zircon dating by selection of more concordant fractions using a high gradient magnetic separation technique. Geochim Cosmochim Acta 46:631-635
Krylov DP, Zagnitko VN, Hoernes S, Lugovaja IP, Hoffbauer R (2002) Oxygen isotope fractionation between zircon and water: Experimental determination and comparison with quartz-zircon calibrations. Eur J Mineral 14:849-853
Lackey JS, Valley JW, Saleeby JB (2003) Evidence from zircon for high $\delta^{18}O$ contamination of magmas in the deep Sierra Nevada Batholith, California. Geology (in review)
Lackey JS, Hinke HJ, Valley JW (2002) Tracking contamination in felsic magma chambers with $\delta^{18}O$ of magmatic garnet and zircon. Goldschmidt Conf, Extended Abstr, Geochim Cosmochim Acta 66, Supplement 1:428
Lackey JS, Valley JW, Chen JH (2001) Correlated O-Sr-Pb isotope ratios in the West-Central Sierra Nevada Batholith, California. Geol Soc Am Abstr Progr 33:295
Larson PB, Geist DJ (1995) On the origin of low-^{18}O magmas: Evidence from the Casto pluton, Idaho. Geology 23:909-912
Lipman PW, Friedman I (1975) Interaction of meteoric water with magma: an oxygen-isotope study of ash-flow sheets from southern Nevada. Geol Soc Am Bull 86:695-702
Masi U, O'Neil JR, Kistler RW (1981) Stable isotope systematics in Mesozoic granites of central and northern California and southwestern Oregon. Contrib Mineral Petrol 76:116-126
Mattey D, Lowry D, Macpherson C (1994) Oxygen Isotope Composition of Mantle Peridotite. Earth Planet Sci Lett 128:231-241
McKeegan KD, Leshin LA (2001) Stable isotope variations in extraterrestrial materials. *In* Valley JW, Cole DR (eds) Stable Isotope Geochemistry. Rev Mineral Geochem 43:279-318
McLelland J, Daly JS, McLelland JM (1996) The Grenville orogenic cycle (ca. 1350-1000 Ma): An Adirondack perspective. Tectonophysics 265:1-28
Mojzsis SJ, Harrison TM, Pidgeon RT (2001) Oxygen-isotope evidence from ancient zircons for liquid water at the Earth's surface 4,300 Myr ago. Nature 409:178-181
Monani S, Valley JW (2001) Oxygen isotope ratio of zircon: magma genesis of low $\delta^{18}O$ granites from the British Tertiary Igneous Province, western Scotland. Earth Planet Sci Lett 184:377-392
Morrison J, Valley JW (1988) Contamination of the Marcy anorthosite massif, Adirondack Mountains, NY: Petrologic and isotopic evidence. Contrib Mineral Petrol 98:97-108
Muehlenbachs K, Kushiro I (1974) Measurements of oxygen diffusion in silicates. EOS Trans Am Geophys Union 56:459
Nasdala L, Wenzel M, Vavra G, Irmer G, Wenzel T, Kober B (2001) Metamictization of natural zircon: accumulation versus thermal annealing of radioactivity-induced damage. Contrib Mineral Petrol 141:125-144

O'Connor YL, Morrison J (1999) Oxygen isotope constraints on the petrogenesis of the Sybille Intrusion of the Proterozoic Laramie anorthosite complex. Contrib Mineral Petrol 136:81-91
Peck WH (2000) Oxygen Isotope Studies of Grenville Metamorphism and Magmatism. PhD dissertation, University of Wisconsin-Madison, 320 p
Peck WH, Valley JW (2000) Large crustal input to high $\delta^{18}O$ anorthosite massifs of the southern Grenville Province: new evidence from the Morin Complex, Quebec. Contrib Mineral Petrol 139:402-417
Peck WH, King EM, Valley JW (2000) Oxygen isotope perspective on Precambrian crustal growth and maturation. Geology 28:363-366
Peck WH, Valley JW, Graham CM (2003a) Slow oxygen diffusion rates in igneous zircons from metamorphic rocks. Am Mineral (in press)
Peck WH, Valley JW, Corriveau L, Davidson A, McLelland J, Farber D (2003b) Mapping terrane boundaries in the deep crust of the Grenville Province using oxygen isotope ratios of zircon from anorthosite-suite granitoids. *In* Proterozoic Evolution of the Grenville Orogen in North America. Geol Soc Am Memoir (in press)
Peck WH, Valley JW, Wilde SA, Graham CM (2001) Oxygen isotope ratios and rare earth elements in 3.3 to 4.4 Ga zircons: Ion microprobe evidence for high $\delta^{18}O$ continental crust and oceans in the Early Archean. Geochim Cosmochim Acta 65:4215-4229
Reischmann T (1995) Precise U/ Pb age determination with baddeleyite (ZrO_2), a case study from the Phalaborwa igneous complex, South Africa. S African J Geol 98:1-4
Richter R, Hoernes S (1988) The application of the increment method in comparison with experimentally derived and calculated O-isotope fractionations. Chemie Erde 48:1-18
Ross DC (1983) Generalized geologic map of the southern Sierra Nevada, California, showing the location of basement samples for which whole rock $\delta^{18}O$ has been determined. U S Geol Survey Open-File Report 83-0904, 1 sheet, 1:250,000
Rudashevsky NS, Burakov BE, Lupal SD, Thalhammer OAR, Saini-Eidukat B (1995) Liberation of accessory minerals from various rock types by electric-pulse disintegration-method and application. Trans Min Metall 104:C25-C28
Rumble D, Giorgis D, Ireland T, Zhang Z, Xu H, Yui TF, Yang J, Xu Z, Liou JG (2002) Low $\delta^{18}O$ zircons, U-Pb dating, and the age of the Qinglongshan oxygen and hydrogen isotope anomaly near Donghai in Jiangsu Province, China. Geochim Cosmochim Acta 66:2299-2306
Saint-Eidukat B, Weiblen PW (1996) A new method of fossil preparation, using high-voltage electric pulses. Curator 39:139-144
Sessions AL, Brady JB, Chamberlain CP (1996) Experimental calibration of an oxygen isotope fractionation factor for zircon. Geol Soc Am Abstr Progr 28:213
Sessions AL, Brady JB, Chamberlain CP, Rumble D (2003) Experimental measurement of oxygen isotope fractionation between calcite and zircon. Am Mineral (in review)
Sheppard SMF (1986) Igneous rocks: III Isotopic case studies of magmatism in Africa, Eurasia and oceanic islands. Rev Mineral 16:319-371
Shieh YN (1985) High-^{18}O granitic plutons from the Frontenac Axis, Grenville Province of Ontario, Canada. Geochim Cosmochim Acta 49:117-123
Shirey SB, Hanson GN (1984) Mantle-derived Archaean monzodiorites and trachyandesites. Nature 310:222-224
Sial AN, Toselli AJ, Saavedra A, Parada MA, Ferreira VP (1999) Emplacement, petrological and magnetic susceptibility characteristics of diverse magmatic epidote-bearing granitoid rocks in Brazil, Argentina and Chile. Lithos 46:367-392
Silver LT (1963) The use of co-genetic uranium-lead isotope systems in zircons in geochronology. *In* Radioactive Dating. Intl Atomic Energy Agency, Symp Proc, Athens, p 279-287
Smyth JR (1989) Electrostatic characterization of oxygen sites in minerals. Geochim Cosmochim Acta 53:1101-1110
Solomon GC, Taylor HP (1989) Isotopic evidence for the origin of Mesozoic and Cenozoic granitic plutons in the northern Great Basin. Geology 17:591-594
Speer JA (1982) Zircon. Rev Mineral 5:67-112
Stern RA, Hanson GN (1991) Archean high-Mg granodiorite: A derivative of light rare earth element-enriched monzodiorite of mantle origin. J Petrol 32:201-238
Stern RA, Hanson GN, Shirey SB (1989) Petrogenesis of mantle-derived, LILE-enriched Archean monzodiorites and trachyandesites (sanukitoids) in southwestern Superior Province. Can J Earth Sci 26:1688-1712
Taylor BE, Huston DL (1998) Hydrothermal alteration of oxygen isotope ratios in quartz phenocrysts, Kidd Creek Mine, Ontario: Magmatic values preserved in zircons: comment. Geology 26:763-764
Taylor BE, Huston DL (1999) Regional $\delta^{18}O$ zoning and hydrogen isotope studies in the Kidd Creek volcanic complex, Timmins, Ontario. *In* Harrington MD, Barrie CT (eds) The giant Kidd Creek volcanogenic massive sulfide deposit, western Abitibi Subprovince, Canada. Econ Geol 10:351-378
Taylor HP (1969) Oxygen isotope studies of anorthosites, with particular reference to the origin of bodies in the Adirondack mountains, New York. *In* Isachsen Y (ed) Origin of Anorthosite and Related Rocks. New York State

Museum 18:111-134
Taylor HP (1986) Igneous rocks: II. Isotopic case studies of circumpacific magmatism. Rev Mineral 16:273-317
Taylor HP, Sheppard SMF (1986) Igneous rocks I. Processes of isotopic fractionation and isotope systematics. Rev Mineral 16:227-271
Upton BGJ, Hinton RW, Aspen P, Finch A, Valley JW (1999) Megacrysts and Associated Xenoliths: Evidence for Migration of Geochemically Enriched Melts in the Upper Mantle beneath Scotland. J Petrol 40:935-956
Valley JW, O'Neil JR (1984) Fluid Heterogeneity during Granulite Facies Metamorphism in the Adirondacks: Stable Isotope Evidence. Contrib Mineral Petrol 85:158-173
Valley JW, Graham CM (1991) Ion microprobe analysis of oxygen isotope ratios in metamorphic magnetite-diffusion reequilibration and implications for thermal history. Contrib Mineral Petrol 109:38-52
Valley JW, Graham CM (1993) Cryptic grain-scale heterogeneity of oxygen isotope ratios in metamorphic magnetite. Science 259:1729-1733
Valley JW, Graham CM (1996) Ion microprobe analysis of oxygen isotope ratios in quartz from Skye granite: healed micro-cracks, fluid flow, and hydro-thermal exchange. Contrib Mineral Petrol 124: 225-234
Valley JW, Taylor HP, O'Neil JR (eds) (1986) Stable Isotopes in High Temperature Geological Processes. Reviews in Mineralogy, Vol. 16, 570 p
Valley JW, Chiarenzelli J, McLelland JM (1994) Oxygen Isotope Geochemistry of Zircon. Earth Planet Sci Lett 126:187-206
Valley JW, Bindeman IN, Peck WH (2003) Empirical calibration of oxygen isotope fractionation in zircon. Geochim Cosmochim Acta (in press)
Valley JW, Kinny PD, Schulze DJ, Spicuzza MJ (1998b) Zircon Megacrysts from Kimberlite: Oxygen isotope heterogeneity among mantle melts. Contrib Mineral Petrol 133: 1-11
Valley JW, Peck WH, King EM, Wilde SA (2002) A cool early Earth. Geology 30:351-354
Valley JW, Graham CM, Harte B, Kinny P, Eiler J M (1998a) Ion microprobe analysis of oxygen, carbon, and hydrogen isotope ratios. Rev Econ Geol 7:73-98
Valley JW, Kitchen NE, Kohn MJ, Niendorf CR, Spicuzza MJ (1995) UWG-2, A garnet standard for oxygen isotope ratio: strategies for high precision and accuracy with laser heating. Geochim Cosmochim Acta 59:5223-5231
Wang DZ, Zhao GT, Qiu JS (1995) The tectonic constraint on the late Mesozoic A-type granitoids in eastern China. Geological J China Univ 1:13-21
Wasteneys H, McLelland J, Lumbers S (1999) Precise zircon geochronology in the Adirondack lowlands and implications for revising plate-tectonic models of the Central Metasedimentary belt and Adirondack Mountains, Grenville Province. Can J Earth Sci 36:967-984
Watson EB (1996) Dissolution, growth and survival of zircons during crustal fusion: kinetic principles, geological models and implications for isotopic inheritance. Trans R Soc Edinburgh 87:43-56
Watson EB, Cherniak DJ (1997) Oxygen diffusion in zircon. Earth Planet Sci Lett 148:527-544
Wei CS, Zheng YF, Zhao ZF, Valley JW (2002) Oxygen and neodymium isotope evidence for recycling of juvenile crust in northeast China. Geology 30:375-378
Wei CS, Valley JW, Zheng YF, Zhao ZF, Spicuzza MJ (2003) origin of low $\delta^{18}O$ magma: Zircon evidence of A-type granites in eastern China. (in review)
Wiechert U, Fiebig J, Przybilla R, Xiao Y, Hoefs J (2002) Excimer laser isotope-ratio-monitoring mass spectrometry for *in situ* oxygen isotope analysis. Chem Geol 182:179-194
Wiedenbeck M, Allé P, Corfu F, Griffin WL, Meier M, Oberli F, Von Quadt A, Roddick JC, Spiegel W (1995) Three natural zircon standards for U-Th-Pb, Lu-Hf, trace element and REE analyses. Geostandards Newslett 19:1-23
Wilde SA, Valley JW, Peck WH, Graham CM (2001) Evidence from detrital zircons for the Existence of continental crust and oceans on the Earth 4.4 Gyr ago. Nature 409:175-178
Wilson CJN, Hildreth W (1997) The Bishop Tuff: New insights from eruptive stratigraphy. J Geol 105:407-439
Wopenka B, Jolliff BL, Zinner E, Kremser DT (1996) Trace element zoning and incipient metamictization in a lunar zircon: application of three microprobe techniques. Am Mineral 81:902-912
Wu FY, Jahn BM, Wilde SA, Sun DY (2000) Phanerozoic continental growth: Sr-Nd isotopic evidence from the granites of northeastern China. Tectonophysics 328:89-113
Wu FY, Sun DY, Li H, Jahn BM, Wilde S (2002) A-type granites in northeastern China: Age and geochemical constraints on their petrogenesis. Chem Geol 187:143-173
Zartman RE (1974) Lead isotopic provinces in the Cordillera of western United States and their geologic significance. Econ Geol 69:792-805
Zheng YF (1993) Calculation of oxygen isotope fractionation in anhydrous silicate minerals. Earth Planet Sci Lett 120:247-263
Zheng YF, Fu B (1998) Estimation of oxygen diffusivity from anion porosity in minerals. Geochem J 32:71-89
Zheng YF, Gong B, Chen F-K (2003) Evidence from magmatic zircons for Neoproterozoic meteoric-hydrothermal alteration and snowball Earth event. (unpublished manuscript)